RAWINSONDE ERRORS AND THEIR APPLICATION TO A MESOSCALE STUDY

by

Bruce Alan Clark

# United States Naval Postgraduate School

# THESIS

RAWINSONDE ERRORS AND THEIR APPLICATION
TO A MESOSCALE STUDY

by

Bruce Alan Clark



October 1969

Rawinsonde Errors and Their Application
to a Mesoscale Study

by

Bruce Alan Clark
Lieutenant Commander, United States Navy
B.S., United States Naval Academy, 1956

Submitted in partial fulfillment of the
requirements for the degree of

MASTER OF SCIENCE IN METEOROLOGY

from the

NAVAL POSTGRADUATE SCHOOL
October 1969

## ABSTRACT

Several studies of rawinsonde component errors in actual flight tests are discussed. RMS relative errors between radiosondes are assumed for measured parameters. These errors are then used to derive RMS relative errors for other parameters such as wind speed and direction, height, virtual temperature, and mixing ratio. Expected RMS errors in measured and derived parameters are discussed in relation to the data obtained from the Oklahoma National Severe Storms Laboratory upper-air mesonetwork. It is found that many analyses and computations which are useful in synoptic-scale meteorology are not practical on the mesoscale. Wind data, when processed by computer, yield the most valid results.

TABLE OF CONTENTS

## LIST OF TABLES

## LIST OF ILLUSTRATIONS

## LIST OF SYMBOLS AND ABBREVIATIONS

| | |
|---|---|
| ATC | Advective temperature change |
| $c_p$ | Specific heat at constant pressure |
| D | Horizontal displacement of radiosonde |
| e | Vapor pressure |
| $e_s$ | Saturated vapor pressure |
| E | Elevation angle |
| g | Acceleration due to gravity |
| h | Thickness (of a layer) |
| j | Joules |
| L | Latent heat of condensation |
| m | Mixing ratio |
| m $sec^{-1}$ | Meters per second |
| mb | Millibars |
| mc | Megacycle |
| $m_s$ | Saturated mixing ratio |
| M | Montgomery stream function |
| nm | Nautical mile |
| p | Pressure |
| q | Specific humidity |
| r | Balloon radius |
| R | Dry gas constant |
| Re | Reynolds number |
| RH | Root mean square (see $\sigma$) |
| SE | Static energy |

| | |
|---|---|
| SR | Slant range |
| $t$ | Time |
| $T$ | Temperature |
| $t_d$ | Dew-point temperature |
| $t_v$ | Virtual temperature |
| TE | Total energy |
| $V$ | Wind speed |
| $V_g$ | Geostrophic wind speed |
| $z, Z$ | Height |
| $\theta_v$ | Potential virtual temperature |
| $\mu$ | Viscosity of air |
| $\rho$ | Density |
| $\sigma$ | Standard deviation or RMS |

# I. INTRODUCTION

For several years the National Severe Storms Laboratory (NSSL) of ESSA has taken mesoscale observations and conducted research in an attempt to better understand the processes involved in severe local storms and therefore enable them to predict storm occurrence more accurately. In 1967 upper-air data were obtained by serial rawinsonde ascents from each of nine stations in the southern Oklahoma mesonetwork on those days when severe storms were likely to occur in the area. GMD-1 Rawin Sets were utilized to track the standard Weather Bureau radiosondes utilizing lithium chloride humidity elements. All soundings were terminated at 100 mb to insure a 90 minute interval between ascents. Data reduction was accomplished by computer utilizing essentially the same program as used for Project Stormy Spring documented by Kreitzberg and Brockman (1966).

Using data provided by NSSL for three days in April and May, 1967, several graduate students at the Naval Postgraduate School have undertaken research projects to gain additional knowledge of atmospheric motions of this scale (cf. Anawalt, 1969; Van Sickle, 1969; Coleman, 1969). All have encountered difficulty in analyzing the rawinsonde data. Analysis of mesoscale upper-air data is new relative to synoptic-scale analysis in meteorology, and there seems to be no proven techniques which apply to this scale. Attempts to apply synoptic-scale procedures have often failed or led to doubtful results. One cannot assume that the wind field is geostrophic or that balance equations, useful on a synoptic scale, will be valid. Also, gradients of moisture

and temperature are expected to be highly nonlinear and much larger than is commonly measured using synoptic-scale data. The main problem in analysis is: how much should the analyst smooth the data and still be reasonably certain of retaining significant features?

At least part of the difficulty in analysis may be attributed to errors in rawinsonde measurements. In this case one is not so interested in total error in temperature, pressure, and relative humidity as in the relative error or dispersion between two identical instruments as they would measure the same parameters. Since the upper-air mesonetwork as it existed in 1967 had as average distance between stations of 85 km (46 nm), the differences in both measured and derived parameters between stations sometimes result in unexpectedly large gradients. An attempt was made to discover what part of these gradients was attributable to real meteorological differences and what portion was caused by relative errors between radiosondes.

Sources of error and the results of several tests of radiosonde accuracy were studied and are discussed in Section II. Some of the factors which principally affect the total error are briefly mentioned. Standard deviations of temperature, pressure, and relative humidity between two similar radiosondes measuring these parameters at the same time and place are assumed. The standard deviation of relative error is defined as: $\sigma=\sqrt{\frac{\Sigma x^2}{N}}$, where $\sigma$ is the standard deviation and alternatively referred to as the root mean square (RMS) error, $\Sigma x^2$ is the sum of the squares of the differences, and N is the number of measurements of x. Resultant errors in derived data such as heights and mixing ratios are developed in Section III with the errors in wind data applicable to the synoptic network in the United States. Finally,

these expected RMS errors in measured and derived parameters are discussed in relation to the data obtained at the Oklahoma NSSL network. Computations and analyses which are useful on a synoptic scale are investigated for use on this mesoscale.

The content of this thesis represents two main research objectives. They are:

1. To develop an appreciation for the magnitudes of RMS relative errors in rawinsonde data as obtained from both the synoptic network and the NSSL mesonetwork.
2. To discover what analyses and computations commonly applied to synoptic-scale data would be useful on this mesoscale.

## II. EVALUATION OF RAWINSONDE COMPONENT ERRORS

### A. PRESSURE

In the technical report, Accuracies of Radiosonde Data (1955), the Air Weather Service listed several sources of error and the tolerances for each in terms of standard deviation which were derived from flight similitude tests. Sources of error itemized were standard barometer, operating standard barometer, accuracy of pressure element, temperature effect, station barometer, and error in estimating fractional contacts. The standard deviations assumed for each of the above sources were statistically combined to give an expected total standard deviation of $\pm$ 2.12 mb up to 15 km (about 100 mb) for each radiosonde. A Signal Corps study of actual flight tests reported in the same publication resulted in a standard deviation of $\pm$ 3.75 mb up to 15 km with smaller errors above that altitude. A value commonly ascribed to the standard deviation of pressure errors in a tropospheric sounding has been $\sigma_p = \pm 3.0$ mb. This value was used in this report by the Air Weather Service to compute height errors up to 100 mb.

More recent investigations have shed some light on several possible sources of error. Hodge and Harmantas (1965) reported up to 3 mb difference for 16 standard Weather Bureau radiosondes between the original factory calibration and a recalibration at room temperature in the Weather Bureau laboratory. The recalibration of a like number of military AN/AMT-4B radiosondes revealed up to 6 mb difference. Most of the radiosondes tested, 95% of the Weather Bureau and 85% of the military, fell within $\pm$ 2 mb. Some of these radiosondes were recalibrated

at a temperature 80 degrees colder than room temperature (about -55C) and the difference in pressure between warm and cold recalibration varied up to a maximum of 5 mb. Supposedly the baroswitch is temperature compensated, but this is clearly inadequate.

Since both the Weather Bureau and AN/AMT-4B radiosondes carry their batteries internally, this introduces a heat source to the other radiosonde components. Andersen (1966) tested the heat buildup by placing a thermocouple one centimeter from the center of the interior of the baroswitch diaphram and measuring baroswitch and environment temperature in a home freezer while a small electric fan prevented stratification. When these temperatures stabilized, the environment temperature was -28C and the baroswitch of the AN/AMT-4B was 0C. This would imply that the baroswitch and, to some extent, the humidity element and thermistor would remain at some temperature which is warmer than the environment in a normal sounding of the troposphere.

Corbeille (1966) compared the AN/AMT-4B with the AN/AMT-11 (a 403 mc radiosonde used aboard Navy ships) in 50 flights of two radiosondes each. Spurious superadiabatic lapse rates found in his investigation were attributed to lag in the baroswitch of the AN/AMT-11. These lapse rates occurred between 400 mb and the tropopause over a time interval of one or two minutes. The lapse rates were not verified by the AN/AMT-4B trace even though the pressure did not decline at a steady rate. However, the AN/AMT-11 uses an externally mounted battery while the AN/AMT-4B, like the Weather Bureau radiosonde, uses an internally mounted battery. The theory advanced is that the heat from the battery compartment of the AN/AMT-4B which keeps the baroswitch much warmer than that of the AN/AMT-11 may cause errors due to temperature but at

the same time lessens the lag due to friction of the contact arm on the commutator bar and prolongs the relatively smooth functioning of the baroswitch.

The pressure difference between the AN/AMT-4B and the AN/AMT-11 was computed each minute of 15 flights by Corbeille (1966). The AN/AMT-4B had a mean pressure 2.0 mb lower than the AN/AMT-11C, and a standard deviation from the mean of 0.9 mb resulted. The mean differences were evaluated at three minute intervals and showed a range of -3.5 to + 2.0 mb. Hodge and Harmantas (1965) computed the root mean square of the pressure differences taken at one minute intervals for 16 flights of the Weather Bureau and AN/AMT-4B radiosondes. This standard deviation was 2.1 mb for all 16 flights and ranged from 1.1 to 3.1 mb for each flight. The maximum pressure difference of 7.0 mb occurred twice in the lower troposphere.

## B. TEMPERATURE

In the publication Accuracies of Radiosonde Data (1955) the Air Weather Service synthesized four studies of temperature errors including radiosonde comparisons by New York University and the Oklahoma City tests by the Weather Bureau in 1951. Assuming that errors were normally distributed around zero, the standard deviation of temperature error was computed at standard pressure levels and ranged from 0.65C to 1.3C in the troposphere for the NYU study. The Oklahoma City tests showed a standard deviation of 0.82C for all standard pressure surfaces from the surface up to 400 mb and 0.99C from 300 mb to 100 mb. It should be noted that this data represents the errors to be expected in a one instrument sounding, and therefore two instruments of the same kind

flown together would have a standard deviation of their differences of 1.414 times the standard deviation of a one-instrument sounding according to $\sigma_{x-y} = \sqrt{\sigma_x^{\ 2} + \sigma_y^{\ 2}}$. Also, the data includes errors in pressure proportional to the baric lapse rate. This error source will be investigated more fully in Section III.

It has been common practice by analysts to assume a standard deviation of 1C for upper-air temperature data on isobaric charts. This is close to the results of all but the most recent studies. Corbeille (1966) in comparing the AN/AMT-4B and the AN/AMT-11C found that in some soundings temperature differences greater than 5C existed, but the majority of soundings contained differences of less than 3C. The AN/AMT-4B was biased toward warmer temperature with the mean value of the differences being 0.6C and a standard deviation from that mean of 0.9C. These figures should not be strictly applied to the Weather Bureau radiosonde because, as mentioned before, the AN/AMT-4B, like the Weather Bureau radiosonde, has an internal heat source while the AN/AMT-11C does not. Also slight difference in thermistors existed between the two radiosondes. However, the results are compatible with an assumed standard deviation of 1C for each instrument.

Air Weather Service Pamphlet 105-3 (1967) specifies a RMS accuracy of 0.7C for the temperature element in the AN/AMT-4, the Weather Bureau radiosonde and the AN/AMT-12 (which contains a hypsometer and is sometimes used by the U. S. Air Force). This would indicate an expected RMS error of about 1C between two radiosondes on the same flight; but this value applies up to 36 km which is considerably higher than the tropopause, the limit of interest for this study. Daniels (1968), Reynolds and Lamberth (1966), Ney et. al (1961), and Badgley (1957)

indicate that radiation errors, lag constants, ventilation rates, and configuration effects contribute more to temperature measurement errors with an increase in altitude and considerably affect the total accuracy. Since relative accuracy is of interest here, one would expect somewhat less error if soundings were limited to 100 mb (about 15 km).

Hodge and Harmantas (1965) computed the RMS differences for each minute of 16 flights which resulted in a RMS value of 0.51C for all flights and a range of 0.38C to 0.87C for each sounding. The temperature differences at the mandatory pressure levels were also computed with 53% of the daytime differences and 52% of the nighttime differences within $\pm$ 0.5C. These figures result in a standard deviation of 0.7C for the standard isobaric levels. The standard deviations of 0.5C at the same time and 0.7C at the same isobaric level were considerably better than one would expect which indicates that differences between compatible instruments are much less than the total error of the instrument.

C. RELATIVE HUMIDITY

The lithium chloride humidity element was being phased out in favor of the carbon element, but it was the LiCl element which was used in the radiosondes at the Oklahoma NSSL network in 1967. Major shortcomings ascribed to the LiCl element are insensitivity, large lag constants, and the reluctance to measure high humidities in the presence of rain or cloud droplets. O'Conner (1952) indicated that relative humidity is measured with respect to water; and, therefore, lower readings should be expected in cirrus clouds. In that case 70-80% relative humidity may be accurate. For example, at -20C 83% RH with

respect to water is equivalent to 100% RH with respect to ice. Also, condensation on the element leads to error at the time of occurrence and during the rest of the sounding. Mathews (1964) ascribes the low readings in clouds to an exothermic liberation of heat in the lithium chloride film as it absorbs moisture.

Mathews (1964) summarized the development of the lithium chloride hygrometer and presented the testing specifications required of the manufacturer. By 1962 all elements were tested at room temperature to $\pm$ 3% of a reference relative humidity. Four out of 100 were tested against the standard calibration between 20% and 95% ascending and descending relative humidity at eight points. Errors were not to exceed 7% RH at one point and 5% at all other points. One out of 100 elements were tested for polarization by switching it on for 15 seconds and then off for 30 seconds for a total of 30 minutes at a constant relative humidity. Maximum drift allowable was 6% relative humidity. One element out of 1,000 was tested for time lag by decreasing the relative humidity from 90% to 40% and allowing a maximum of 15 seconds for 90% of the change with a wind speed of 250 meters per minute (the approximate ascent rate of the standard radiosonde). The first three test specifications indicate a standard deviation of those errors combined to be about 3% relative humidity at room temperature.

Large lag constants would cause large errors in relative humidity especially if the relative humidity were changing rapidly. Mathews (1964) also reported a study of low temperature lag characteristics done by Jones and Wexler (1960). At a wind speed of 160 meters per minute the response time to accomplish a 63% (1 - 1/e) change in relative humidity ranged from 51 to 74 seconds at -20C and 120 to 480

seconds at -40C. Ference (1951) reported response times of four seconds at -25C, 15 seconds at 0C, and 120 seconds at -30C. This implies that at 500 mb and higher this element may indicate relative humidities which were sensed hundreds of meters below. For computations at standard pressure levels or even averaging over small layers the lag of the lithium chloride hygrometer may cause relatively large errors.

It has been standard practice by analysts to assume a standard deviation of ± 5% RH for temperatures above 0C and ± 10% between 0C and -40C. The corresponding standard deviation of the difference between two instruments on the same sounding would therefore be 7% and 14% respectively. Hodge and Harmantas (1965), using the carbon element in the AN/AMT-4B and the lithium chloride element in the Weather Bureau radiosonde, found that 79% of the differences at each minute were within ± 10% RH. This figure converted to a normal curve results in a standard deviation of 8% RH. Corbeille (1966) reported essentially the same overall results with the errors increasing with decreasing pressure. Unfortunately there have been no tests in the last decade with two lithium chloride hygrometers in the same flight. Therefore a standard deviation between two sensors of 5% RH above 0C and 10% RH below 0C will be assumed.

## D. WIND MEASUREMENT

Wind is commonly measured by tracking the radiosonde in its ascent by a GMD-1 Rawin Set and recording azimuth and elevation angles at set time intervals. The height of the radiosonde is computed from the integration of the hypsometric equation; and by using azimuth and elevation angles, the position of the instrument over the curved earth

is thus determined. By comparing two positions at either end of an elapsed time one arrives at a mean wind speed and direction for the layer represented by the heights of the radiosonde at either end of the time interval. GMD-1 wind data are not reported when the elevation angle is less than six degrees above the horizon or any prominent object or when the azimuth angle is within six degrees of any prominent object on the horizon because of reflected or refracted signals. The RMS accuracy of GMD-1 elevation and azimuth angles is thought to be $\pm$ 0.5 degrees (cf. Danielsen and Duquet, 1966).

The accuracy of the wind obtained from such measurements or from measurements of any free balloon is directly related to the validity of two rather gross assumptions. The first assumption is that the balloon responds completely to the action of the wind. That is, no relative motion exists between the balloon and the air mass except that provided by the balloon's ascent. Consider what happens to the balloon as it encounters changing winds in its ascent. Naturally the balloon trains' mass, momentum, and aerodynamic drag and the air density and vertical shear of the wind are factors which must be considered in determining how fast the balloon train does attain a negligible horizontal relative motion. Near a jet stream the vertical shear is large enough to cause some wind errors, but elsewhere the errors of this type could be considered negligible.

In the last decade there has been increased interest in small scale fluctuations of the wind because of its importance in launching rockets and space probes. As a result there have been many studies of balloon motion relative to the air and another type of error has been brought to light. There exists a self-induced balloon motion which has been

described as both a regular spiral or perturbation vector about a mean wind vector and highly erratic depending upon Reynolds number (cf. MacCready, 1965). Reynolds number is defined as Re = $2\rho Vr/\mu$, where $\rho$ is the density of air, $\mu$ is the viscosity, V is the speed of air relative to the balloon, and r is the balloon radius (Scoggins, 1965). With supercritical Reynolds number the motion is erratic while subcritical Re permits more regular balloon oscillations.

Murrow and Henry (1965) investigated the behavior of several types and sizes of balloons including the standard radiosonde balloon in still air inside a 220 foot high blimp hanger at Lakehurst, New Jersey. They concluded that horizontal velocity was about one-half the vertical velocity, and that large roughness elements added to a balloon surface resulted in reduced amplitudes of horizontal motion and reduced wavelengths of this motion in the vertical. Scoggins (1965) investigated the behavior of ROSE and JIMSPHERE balloons and concluded that increasing the number of large roughness elements on the JIMSPHERE reduced the oscillations. McVehil, Pilié, and Zigrossi (1965) used doppler radar to confirm that the type of oscillations of one- and two-meter spherical balloons are dependent upon Reynolds number. MacCready (1965) summarized previous work. He suggests the use of the JIMSPHERE to define small scale variations in the wind field from the surface to 18-20 km. The standard radiosonde should go through a critical Reynolds number regime between 8 and 12 km to a subcritical regime where oscillations become more regular.

Lhermitte (1967) utilized doppler radar in his study of balloon motion. In 45 flights he used neoprene balloons of diameters from 0.3 to about two meters. His conclusions imply that a radiosonde balloon

would develop erratic horizontal displacements of as much as six or eight meters in the supercritical Reynolds number regime (below 8 km according to MacCready (1965)). At higher altitudes in the subcritical regime balloon displacements were regular and about the same amplitude as the balloon diameter (about 3 meters) and the vertical wavelength would be about 50 meters. Therefore, the winds derived from radiosonde measurements averaged over two minutes (about 600 meters in height) are relatively unaffected by the horizontal motions, but they only reveal the gross features of the wind field. As the averaging interval decreases these self-induced horizontal motions take on added significance.

The second assumption is that the position of the balloon or radiosonde can be accurately determined. This results in the most error in routine rawinsonde wind reports. The Air Weather Service and Sandia Corporation conducted a series of wind tests in early 1954 at Salton Sea test base. These tests incorporated wind data from the surface to at least 100 mb. Smith (1954) reported the results of those tests. Winds from three askania phototheodolites were used as a standard in six radiosonde flights to test the accuracy of two SCR-584 radars and two GMD-1(A)s. The Askanias' reportedly have a position error of less than three meters at 12 km. Therefore the use of Askania-derived winds as a standard appears logical. Although balloon positions and elevation angles were not compensated for curvature of the earth, the maximum error incurred was reported to be about one m $sec^{-1}$. Balloons were underinflated in an attempt to test accuracies at the lowest elevation angles, but none were read at less than 10 degrees. The standard deviation for wind speed as measured by the two GMD-1(A)s was 2.2 m $sec^{-1}$ for all flights and all altitudes and 3.4 m $sec^{-1}$ at altitudes

above 7.5 km. Standard deviations from all stations were directly correlated with height, slant range, and wind speed.

Danielsen and Duquet (1966) developed and tested a machine method for computing winds from GMD-1 tracking and radiosonde data. FPS-16 precision radar derived winds were used as a standard. The RMS accuracies for the radar are almost one order of magnitude smaller (0.01 degree in elevation and azimuth and five yards in slant range) than GMD-1 and radiosonde accuracies. Radar readouts were obtained 10 times a second to determine small scale variations in elevation and azimuth. Winds were computed over 2, 10, 20, and 40 second averages. The power spectra of the winds revealed a large spectral peak at a period of nine seconds which was attributed to the natural period for self-induced balloon oscillation. The two second averaged winds showed fairly regular oscillations of $\pm$ 2 m sec$^{-1}$. It is interesting to note that the authors had to use 40 second wind averages to eliminate these high frequency oscillations from the 2-second averages, and the 40-second averages were used in later comparison with GMD-1 and radiosonde derived winds.

GMD-1 readings were taken every six seconds which is the maximum rate. Deviations from the mean elevation angle appeared to be 0.2 degrees or four times the commonly accepted standard deviation. To suppress this error the authors suggested that an average over at least six points (36 seconds) was necessary. Actually the wind was computed over an interval equal to the barostat contact interval. This required averaging five or six azimuth and elevation angles near the surface and 10 or 12 at 100 mb. Increasing the number of observations in each average helped to compensate for decreasing accuracy

in height and elevation angles. By using an average elevation angle and height, the distance over the curved earth was computed. With this distance and average azimuth angle the position was obtained. Then by taking finite centered differences of successive mid-point positions the winds were calculated at each pressure contact. The time interval varied from about 30 seconds to more than 60 seconds.

In one ascent with fairly light winds the GMD-1/radiosonde derived winds were within one m $sec^{-1}$ and two degrees of the FPS-16 winds. For another sounding with a strong (68 m $sec^{-1}$) jet stream the GMD-1/radiosonde winds accurately described the wind field at lower levels; but above the jet core (13 km) and at low elevation angles, errors of three or four m $sec^{-1}$ were evident. Two ascents resulted in elevation angles of less than 10 degrees. Maximum error in elevation angle was 0.7 degrees or $14\sigma$ making it necessary to fit a fourth order polynomial to smooth the elevation angle data in order to compute reasonable winds. The authors concluded that GMD-1 derived winds closely resembled FPS-16 winds when GMD-1 angles were measured 10 times a minute, carefully read and processed by computer, and elevation angles remained more than 10 degrees above the effective horizon.

## III. RESULTANT ERRORS IN DERIVED DATA

It is necessary to assign some RMS error values to relative humidity, temperature, and pressure in order to compute errors in derived data. Again it must be emphasized that these values are not indicative of absolute accuracies but of relative error or the RMS dispersion between Weather Bureau radiosondes measuring the same parameters at the same time and place.

Hodge and Harmantas (1965) concluded that the AN/AMT-4B and the Weather Bureau radiosondes were indeed compatible because differences noted between these two radiosondes were no greater than could be expected from procurements for different years or from different manufacturers for the same agency. Since there have been no recent tests utilizing two Weather Bureau radiosondes on each sounding, this conclusion takes on added significance. One must give their results great consideration in assigning values for further computation. Accordingly, the following RMS relative errors will be utilized in future computations:

| | | |
|---|---|---|
| Temperature: | $\pm$ 0.5C | |
| Pressure: | $\pm$ 2.0 mb | |
| Relative Humidity: | T > OC, $\pm$ 5% | when clear of clouds and precipitation |
| | -40C $\leq$ T $\leq$ )C, $\pm$ 10% | |

### A. TEMPERATURE ERRORS

To discover temperature errors at some standard pressure levels, one must consider the pressure error and the prevailing lapse rate. The additional error at a particular pressure level will be:

$dT_p = \frac{\partial T}{\partial p} \sigma_p$, where $\frac{\partial T}{\partial p}$ = baric lapse rate at the level in question and $\sigma_p$ = RMS error in pressure (2.0 mb). Using a sounding which is representative of conditions in the NSSL mesonetwork at 1830Z 28 May 1967 results in additional errors due to pressure of from 0.17C at 850 mb to 0.46C at 200 mb. Since the lapse rate near 100 mb was essentially zero, there would be no additional correction for the 100 mb pressure level. The total temperature error on a constant pressure surface or at any specified pressure would be $\sigma_{T_p} = \sqrt{(0.5)^2 + (dT_p)^2}$. Hodge and Harmantas (1965) computed RMS temperature errors at standard pressure levels and found the average to be 0.7C. In the lower troposphere the error is probably less while at 200 mb the error is probably more than 0.7C.

B. MOISTURE PARAMETERS

1. <u>Mixing Ratio and Specific Humidity</u>

Since $q = \frac{m}{1+m}$, there exists a small relative error in assuming that q = m. This error is about 1% for a q or m of 10 gm $kgm^{-1}$.

Since $RH = \frac{m}{m_s}$, an error of 5% in RH implies an error in m of 0.05 $m_s$. For example, consider a relative humidity of 50%, temperature of 23C and pressure of 1000 mb corresponding to a $m_s$ of 18.0 gm $kgm^{-1}$. A 5% error in relative humidity corresponds to an error in mixing ratio of 0.9 gm $kgm^{-1}$ and therefore the actual mixing ratio probably lies between 8.1 and 9.9 gm $kgm^{-1}$ and the corresponding dew point from 10.5 to 13.7C. At a relative humidity of 50%, a RMS error of 5% RH results in an error of 10% of the <u>reported</u> mixing ratio; and at 25% RH for subzero temperatures, a RMS error of 10% RH results in an error of 40% of the reported mixing ratio. Thus the error in mixing

ratio or specific humidity is tied to the saturation value - not the reported value.

2. Virtual Temperature

Virtual temperature is defined as:

$$T_v = T(1 + 0.61q),$$

where T is air temperature in degrees Kelvin. If mixing ratio is used in place of specific humidity, virtual temperature can then be written as

$$T_v \doteq T + 0.61mT. \qquad (1)$$

One finds T = 285K and m = 7 gm $kgm^{-1}$ near 750 mb on the sample sounding. Therefore $T_v$ becomes 286.22K or 1.22C higher than the reported temperature. Taking the differential of equation (1) for error analysis:

$$dT_v = dT + 0.61(mdT + Tdm).$$

If one lets the differentials assume the values of the appropriate standard deviations, then $dT = 0.5C = \sigma_T$ and $dm = 0.05m_s = 0.0006$ at $m_s = 12$ gm $kgm^{-1}$. Therefore mdT = 0.0035C and Tdm = 0.171C. Since mdT < < Tdm, that term can be dropped. Even 0.61 Tdm is small (0.104C). If one assumes that $dT_v = \sigma_{T_v}$, then equation (1) now reads $\sigma_{T_v} = 0.5 + 0.104 = 0.604C$. However, $\sigma_T$ is an average over the whole sounding, and in the lower troposphere the dispersion in temperatures is less than average (Hodge and Harmantas, 1965). In the lowest layers of the tropical atmosphere 0.61Tdm may be large enough to increase $\sigma_{T_v}$ significantly, but in mid-latitudes the reduced dispersion in temperature in the lower layers will compensate for errors in mixing ratio in determining virtual temperature. Consequently, in further computations $\sigma_{T_v} = 0.5C$ will be assumed.

3. Dew-Point Temperature

$T_d$, the dew point, depends upon the temperature, pressure, and relative humidity (or mixing ratio) and can be read from the thermodynamic diagram. Mitchell (1967) converted relative humidity errors of the same magnitude assumed here to dew-point errors for each two degrees of temperature from +40C to -40C in increments of 5% relative humidity. Also presented are two nomograms for the temperature ranges 40C above and below freezing based upon interpolation of the tabulated data. In computing dew points, Mitchell assumed that $RH \equiv \frac{m}{m_s} \doteq \frac{e}{e_s}$, and since $e_s$, the saturation vapor pressure, is dependent only upon temperature, his results should be applicable at all pressures.

Using the same sample sounding and Mitchell's tables, RMS errors in dew point are listed in Table I for selected levels.

TABLE I

RMS Error in Dew Point for Sample Sounding

| Pressure (mb) | T ($^oC$) | $T_d(^oC)$ | RMS Error in $T_d(^oC)$ |
|---|---|---|---|
| 950 | 26.4 | 11.6 | $\pm$ 1.9 |
| 850 | 17.2 | 9.6 | $\pm$ 1.3 |
| 700 | 6.0 | -2.9 | $\pm$ 1.3 |
| 500 | -10.5 | -24.2 | $\pm$ 3.6 |
| 300 | -38.3 | -51.9 | $\pm$ 4.3 |

The errors are greatest for high temperatures and low relative humidity in each temperature range. The temperature error would cause an error in $m_s$ and therefore m and $T_d$ at a particular pressure level

apart from the error caused by relative humidity. For example, if the temperature at 700 mb in Table I was in error by 0.7C and the relative humidity remained constant, the reported dew point would be about -3.5C or -2.5C corresponding to a temperature of 5.3C and 6.7C respectively. However, the RMS error in dew point due to errors in relative humidity would remain about the same ($\pm$ 1.3C), and the combined RMS error would be about $\pm$ 1.4C. Therefore the temperature error is of little consequence in determining dew point accuracies and may be considered negligible.

C. HEIGHT OF STANDARD ISOBARIC SURFACES

One must distinguish between the heights of a constant-pressure surface and the height of the radiosonde at the time it indicated that pressure. While both heights are computed in the same manner, the errors in the latter heights are much greater and will be dealt with in the next section.

The heights of constant-pressure surfaces are computed from the hypsometric equation using a mean virtual temperature for the layer. The thickness of each layer is added to the sum of the thicknesses of the layers below to arrive at a height for the top of the layer. The height of the first standard pressure level above mean sea level is computed by the barometric equation with less accuracy but of smaller thickness than the next layer, so that in computing height errors, it is assumed that the 1000 mb height is known exactly. The hypsometric equation which follows is derived from the equation of state for moist air and the hydrostatic equation (Haltiner and Martin, 1957):

$$Z_2 - Z_1 = -\frac{R}{g}\int_1^2 T_v \, \delta(\ln p) \doteq \frac{R}{g}\overline{T_v} \ln \frac{p_1}{p_2}. \qquad (2)$$

The subscripts 1 and 2 represent the bottom and top of the layer respectively and $\overline{T_v}$ is the mean virtual temperature in the layer. By assuming that R and g are constants then the error in thickness of a layer bounded by $p_1$ and $p_2$ will be dependent upon the error in $\overline{T_v}$, the baric lapse rate, $\frac{\partial T}{\partial p}$, assumed constant in the layer, and the standard deviation in pressure measurement, $\sigma_p$. The error in thickness, dh, from Accuracies of Radiosonde Data (1955) is given as

$$dh = \frac{R}{g} \ln \frac{p_1}{p_2} \left( d\overline{T_v} - \frac{\partial T}{\partial p} \sigma_p \right). \qquad (3)$$

1. Error in Thickness Due to Temperature Error

The temperature component of the thickness error is

$$dh_T = \frac{R}{g} \ln \frac{p_1}{p_2} \, d\overline{T_v}. \qquad (4)$$

Since one does not use the virtual temperature at any particular pressure but only the mean $T_v$ in the layer, a standard deviation of 0.5C applies; and the results are shown in Table II.

TABLE II

Standard Deviation in Layer Thickness
Due to Mean Virtual Temperature Error of 0.5C

| Layer (mb) | $dh_T$ (meters) |
|---|---|
| 1000 - 700 | 5.2 |
| 700 - 500 | 4.9 |
| 500 - 300 | 7.5 |
| 300 - 200 | 5.9 |
| 200 - 100 | 10.2 |

If it is assumed that the temperature error maintains the same sign throughout the sounding, the standard deviation in the height of each pressure surface is obtained by adding the thickness errors. Table III gives the results of height error, $\sigma_{hT}$, of several pressure surfaces with only the error in temperature considered.

TABLE III

Standard Deviation in Height of Isobaric Surfaces
Due to Mean Virtual Temperature Error of 0.5C

| Pressure (mb) | $\sigma_{hT}$ (meters) |
|---|---|
| 1000 | 0 |
| 700 | 5.2 |
| 500 | 10.1 |
| 300 | 17.6 |
| 200 | 23.5 |
| 100 | 33.7 |

2. <u>Error in Thickness Due to Pressure Error</u>

The portion of the thickness error due to pressure is

$$dh_p = \frac{R}{g} \ln \frac{p_1}{p_2} \frac{\partial T}{\partial p} \sigma_p . \tag{5}$$

Because the sign of the error is not important in this application, a positive sign is assumed. Notice, however, that if the sign of the lapse rate changes with an otherwise constant pressure error, that the cumulative errors due to pressure would decrease. Using $\frac{\partial T}{\partial p}$ from the sample sounding and $\sigma_p = \pm 2$ mb, Table IV was compiled. In the sample sounding the tropopause occurred at about 150 mb with the

temperature at 200 mb and 100 mb being equal. Since $\frac{\partial T}{\partial p}$ is assumed constant in the layer, there is no error in the 200-100 mb layer; and $\sigma_{hp}$, the additive effect of pressure error on height, in Table V shows the same value for 100 mb at it does for 200 mb.

TABLE IV

Standard Deviation in Layer Thickness Due to a Pressure Error of 2.0 mb

| Layer (mb) | $dh_p$ (meters) |
|---|---|
| 1000 - 700 | 1.7 |
| 700 - 500 | 1.6 |
| 500 - 300 | 4.2 |
| 300 - 200 | 5.4 |
| 200 - 100 | 0 |

TABLE V

Standard Deviation in Height of Isobaric Surfaces Due to a Pressure Error of 2.0 mb

| Pressure (mb) | $\sigma_{hp}$ (meters) |
|---|---|
| 1000 | 0 |
| 700 | 1.7 |
| 500 | 3.3 |
| 300 | 7.5 |
| 200 | 12.9 |
| 100 | 12.9 |

3. Total Error in Height of Isobaric Surfaces

Assuming that temperature and pressure effects are independent of each other and normally distributed $\sigma_h$, the total error in height of a constant-pressure surface in meters, is given by $\sigma_h = \sqrt{(\sigma_{hT})^2+(\sigma_{hp})^2}$. $\sigma_{hT}$ and $\sigma_{hp}$ from Tables III and V are included in Table VI for comparison.

Total error in height at standard constant-pressure surfaces is therefore mostly dependent upon mean virtual temperature errors. The assumption that the temperature and pressure effects on height errors are normally distributed and independent of one another seems

more plausible when one is considering relative errors between two radiosondes than when one is trying to obtain absolute errors.

TABLE VI

Standard Deviation in Height of Isobaric Surfaces (meters) Including Effects of Both Temperature and Pressure Errors

| Pressure (mb) | $\sigma_{hT}$ | $\sigma_{hp}$ | $\sigma_h$ |
|---|---|---|---|
| 1000 | 0 | 0 | 0 |
| 700 | 5.2 | 1.7 | 5.5 |
| 500 | 10.1 | 3.3 | 10.6 |
| 300 | 17.6 | 7.5 | 19.1 |
| 200 | 23.5 | 12.9 | 26.8 |
| 100 | 33.7 | 12.9 | 36.1 |

The true height error in geopotential meters is influenced by several factors which do not affect relative error. The fact that g is considered a constant in the hypsometric equation decreases the height of the 100 mb surface by about 40 meters. However, the fact that the emissivity of the thermistor is near 0.3 on daytime flights probably compensates for the error in g by providing a bias toward warmer than true temperatures (Daniels, 1968; Corbeille, 1966). Also there is a small lag in thermistor response which could increase the temperature beyond the steady-state error (Badgley, 1957). At night the radiation error would cause the thermistor to record lower than ambient temperatures thus increasing the error in true height (Daniels, 1968). While these are some factors which affect the true accuracy to

a considerable extent, one must assume that they are negligible in comparing two radiosondes flown at the same time of day in the same geographical area. One must assume that both thermistors are exposed to equal amounts of solar radiation. Otherwise the radiation error would influence the relative error in temperature between radiosondes. Of more interest are the random errors caused by deviation from standard in manufacture, lock-in errors during the baseline check, proper alignment and readability of the recording equipment, and accuracy of data reduction. These types of errors seemingly are more apt to cause a normal distribution of errors in derived data, because any bias caused by inadequate design is common to all soundings.

## D. HEIGHT OF THE RADIOSONDE

It was shown in Section C that errors in height of the constant-pressure surfaces were caused mostly by temperature errors and only slightly increased by the pressure error coupled with the baric lapse rate. However, if one tries to determine the height of the radiosonde when it indicated a given pressure, then one must consider the error in meters represented by $\sigma_p$ ($\pm$ 2 mb) at the surface in question. For instance, 2 mb in pressure at 500 mb represents 31 meters. However, for the applications considered in this section, one is not interested in relative error between radiosondes but rather that portion of relative error which is attributable to a single radiosonde or $\frac{\sigma_p}{\sqrt{2}}$. From the hydrostatic equation and the equation of state for moist air $dz = -\frac{R\,T_v}{g}\frac{dp}{p}$. Replacing dz and dp by $\sigma_{zp}$ and $\frac{\sigma_p}{\sqrt{2}}$ respectively, this becomes

$$\sigma_{zp} = -\,29.29\,T_v\,\frac{(\pm\sqrt{2})}{p} = \pm\,29.29\,T_v\,\frac{\sqrt{2}}{p}\,. \qquad (6)$$

Using the values for $T_v$ from the sample sounding at the corresponding pressure, the height error corresponding to a $\sqrt{2}$ mb pressure error is obtained. Since wind and significant temperature levels are attributed to the heights of the radiosonde at the time they were measured, this error in height due to error in pressure is frequently encountered. For a single sounding the RMS error in height due to pressure, $\sigma_{zp}$, and the RMS error in height of a constant-pressure surface, $\frac{\sigma_h}{\sqrt{2}}$, are combined to get standard deviation in radiosonde height, $\sigma_z$, by: $\sigma_z = \sqrt{\frac{(\sigma_h)^2}{2} + (\sigma_{zp})^2}$. The results follow in Table VII where RMS errors in some standard isobaric levels are used for $\sigma_h$.

TABLE VII

Standard Deviation (meters) for Height of the Radiosonde at Selected Levels

| Pressure (mb) | $\sigma_{zp}$ | $\frac{\sigma_h}{\sqrt{2}}$ | $\sigma_z$ |
|---|---|---|---|
| 700 | 16.2 | 3.9 | 17.0 |
| 500 | 21.9 | 7.5 | 23.3 |
| 300 | 32.5 | 13.5 | 35.3 |
| 200 | 43.8 | 18.9 | 48.1 |
| 100 | 87.6 | 25.5 | 91.9 |

As can be readily observed from Table VII, the error in pressure is the predominant error in height of the radiosonde. Although stratospheric measurements are beyond the scope of this thesis, it is interesting to note that above 100 mb the pressure error is probably smaller using the conventional barostat; but the error in height due to

pressure error, $\sigma_{zp}$, at 10 mb would be about five times as great as the error at 50 mb. Dowski (1961) showed that barostat-derived heights were fairly accurate in the troposphere with errors commonly about 20 or 30 meters and a maximum error in six flights of 75 meters. However, at an altitude of 30 km, errors as great as 1 km were observed while hypsometer-derived heights at that altitude were generally less than 200 meters in error.

## E. WIND ACCURACY

Suppose one makes some rather gross assumptions in order to make some simple calculations and gain a feeling for the errors in radiosonde position caused by uncertainty in azimuth and elevation angles of the GMD-1. First, assume that the height, z, is known exactly and that the standard deviation of the azimuth and elevation angles is 0.05 degrees. Second, assume that the earth is flat; and, therefore, the effective elevation angle is also the true elevation angle. The representation of a spherical surface by a flat surface results in an error which increases with distance of the radiosonde from the tracking site. For instance, if the radiosonde were displaced 111 km (60 nm), the angle subtended by radii from the earths' center to the tracking site and radiosonde would be one degree causing the elevation angle to read one half of one degree too low. However, elevation angles to be used in this calculation will be 14 degrees and 26.6 degrees with a maximum displacement of 60 km. Therefore, the maximum error in elevation angle is 0.27 degrees.

In Figure 1 the following definitions apply:

D = horizontal displacement

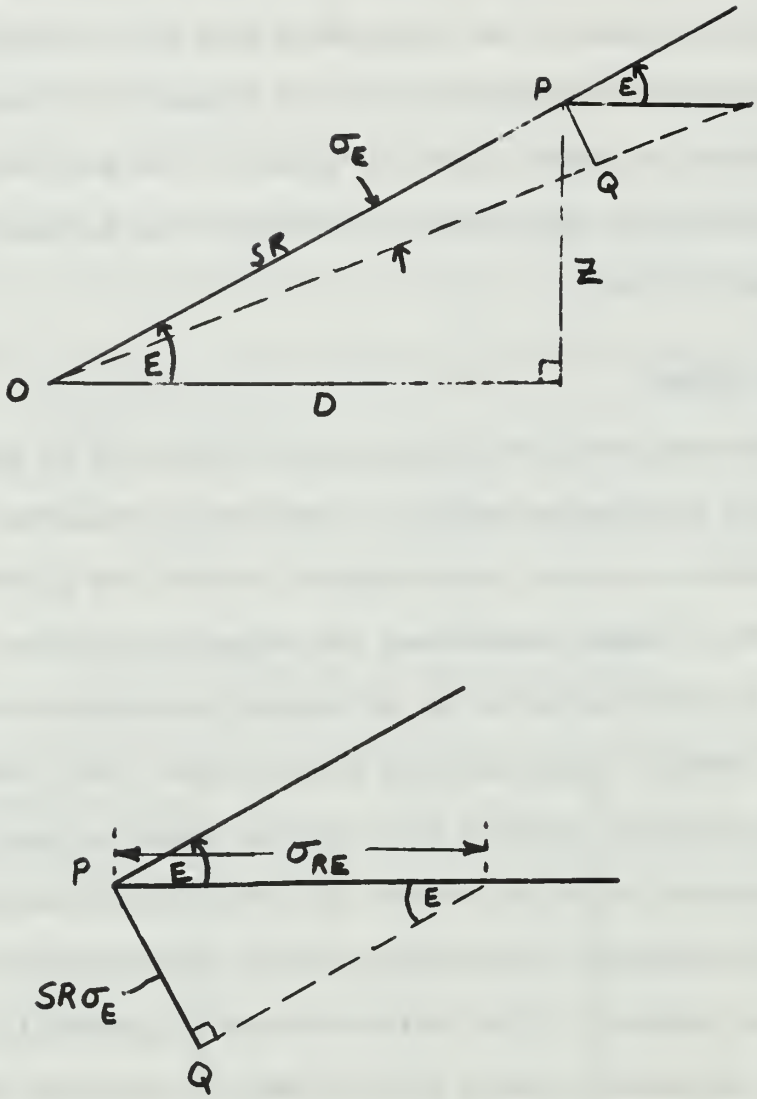


Figure 1: Position Error in Range due to RMS Error in Elevation Angle of GMD-1.

SR = slant range

E = elevation angle

P = position of the radiosonde

Z = height of the radiosonde above the GMD-1

$\sigma_E$ = standard deviation of elevation angle = $0.05^{\circ}$ = 0.00087 radians

$\sigma_{RE}$ = error in range on a horizontal plane due to RMS error in elevation angle

Since Z, E, and $\sigma_E$ are known, one first must find SR. This is given by Z/sin E. Therefore the distance PQ is given by $Z\sigma_E/\sin E$. However, $\sigma_{RE}$, the error in range due to $\sigma_E$ is PQ/sin E. Therefore $\sigma_{RE}$ is

$$\sigma_{RE} = \frac{Z\sigma_E}{(\sin E)^2}. \tag{7}$$

Similarly the error normal to the line of sight is $SR\sigma_A$ and is

$$\sigma_N = \frac{Z\sigma_A}{\sin E}, \tag{8}$$

where $\sigma_A$, the RMS error in azimuth angle, equals $\sigma_E$. Now assume that the ascent rate of the radiosonde is constant at five m $sec^{-1}$. Further, consider two cases where the mean wind speed displacing the radiosonde is 10 and 20 m $sec^{-1}$ so that tanE is 0.5 and 0.25 respectively. $\sigma_{RE}$, $\sigma_N$, and $\sigma_{XG}$, the standard deviation of position error due to GMD-1 measurements, are given for both cases in Table VIII where $\sigma_{XG} = \sqrt{(\sigma_{RE})^2 + (\sigma_N)^2}$.

Since wind is computed by dividing the distance between two positions by the time interval and assuming the errors at the two positions are equal, the standard deviation in wind speed due to GMD-1 errors ($\sigma_{WG}$)

TABLE VIII

Standard Deviation of Position Error (meters)
Due to GMD-1 Measurement Errors

| Mean Wind | | 10 m sec$^{-1}$ | | | 20 m sec$^{-1}$ | | |
|---|---|---|---|---|---|---|---|
| | | $\sigma_{RE}$ | $\sigma_N$ | $\sigma_{XG}$ | $\sigma_{RE}$ | $\sigma_N$ | $\sigma_{XG}$ |
| Z | 5 km | 21.7 | 9.7 | 23.8 | 74 | 17.9 | 76.2 |
| | 10 km | 43.5 | 19.4 | 47.6 | 148 | 35.9 | 152.3 |
| | 15 km | 65.2 | 29.2 | 71.5 | 222 | 53.8 | 228.5 |

can be expressed by

$$\sigma_{WG} = \frac{\sqrt{2}\ \sigma_{XG}}{\Delta t}. \tag{9}$$

Considering the worst case in Table VIII, the standard deviation in wind speed due to GMD-1 errors at 15 km would be 2.7 m sec$^{-1}$ for a two minute interval and 10.8 m sec$^{-1}$ for a 30 second interval.

Up to this point the height (Z) has been considered exact, but this is definitely not the case. To get more realistic values for wind speed errors one must incorporate the errors in range due to errors in height of the radiosonde. Unfortunately these errors in height must be multiplied by the cotangent of the elevation angle to be converted to range errors with the result that low elevation angles compound the problem. Since the errors in height, $\sigma_Z$, and the errors in range due to GMD-1 errors in elevation angle, $\sigma_{RE}$, can be assumed to be independent, the total error in range $\sigma_R$ is given by

$$\sigma_R = \sqrt{(\sigma_{RE})^2 + (\sigma_Z \cot E)^2}. \tag{10}$$

Using values of $\sigma_Z$ interpolated from Table VII and $\sigma_{RE}$ from Table VIII, $\sigma_R$ is computed according to equation (10). Values of $\sigma_N$ are then combined with $\sigma_R$ to get $\sigma_X$, the total standard deviation of position error according to

$$\sigma_X = \sqrt{(\sigma_R)^2 + (\sigma_N)^2}. \tag{11}$$

The standard deviation in wind speed, $\sigma_W$, is then computed by $\sigma_W = \frac{\sqrt{2}\,\sigma_X}{\Delta t}$ with $\Delta t = 2$ minutes, and the results are tabulated in Table IX.

TABLE IX

Standard Deviation of Position Error and Wind Speed
Due to GMD-1 Measurement Errors
and Radiosonde Height Errors (meters)

| Mean Wind | Height | $\sigma_Z$ | $\sigma_Z \cot E$ | $\sigma_{RE}$ | $\sigma_R$ | $\sigma_N$ | $\sigma_X$ (meters) | $\sigma_W$ (m $sec^{-1}$) |
|---|---|---|---|---|---|---|---|---|
| 10 m $sec^{-1}$ | 5 km | 21 | 42 | 21.7 | 47.3 | 9.7 | 48 | 0.57 |
| | 10 km | 36 | 72 | 43.5 | 83.5 | 19.4 | 86 | 1.0 |
| | 15 km | 92 | 184 | 65.2 | 195 | 29.2 | 196 | 2.3 |
| 20 m $sec^{-1}$ | 5 km | 21 | 84 | 74 | 112 | 17.9 | 113 | 1.3 |
| | 10 km | 36 | 144 | 148 | 206 | 35.9 | 209 | 2.5 |
| | 15 km | 92 | 368 | 222 | 430 | 53.8 | 433 | 5.1 |

It is obvious that radiosonde height errors when converted to range errors are predominant in determining wind speed and position errors. This kind of error is minimized by making use of a precision radar to track balloons for upper-wind data. If a FPS-16 were used, all the values in Table VIII would be one-fifth as great. The five-meter standard deviation in slant range must be multiplied by the cosine of

the elevation angle to yield errors in range or displacement of about four meters which may be compared to values of $\sigma_R$ in Table IX. Obviously, if a precision radar is available, it should be used when detailed structure of the wind field is desired.

If one assumes the instantaneous wind speed at a particular level to be 1.5 times the mean wind, then reported wind speeds in the upper troposphere are often in error by $\pm$ 15% and errors in the stratosphere may be in error by $\pm$ 30% or more. This conclusion is based upon the fact that the two mean winds outlined above certainly do not represent extreme conditions but rather conditions which are fairly typical in mid-latitudes.

The problem of ascertaining the RMS error in direction remains. If one assumes that the wind affecting the radiosonde is along the azimuth of the instrument, then the error in direction is a result of only the error in azimuth angle. Given a synoptic situation with a mean wind speed of 10 m $sec^{-1}$ up to 300 mb (10 km) and a wind speed of 15 m $sec^{-1}$ at that level, then the radiosonde would be displaced 1800 meters in two minutes; and the error normal to the wind would be $\sigma_N \sqrt{2}$ or 27.4 meters. Thus the error in direction would be equal to arctan 27.4/1800 or about 0.9 degrees. However, if the wind at 300 mb were perpendicular to the azimuth of the instrument, the error normal to the wind would be $\sigma_R \sqrt{2}$ or 118 meters causing an error in direction of arctan 118/1800 or about 3.3 degrees. The true wind is usually at some angle between these two extremes, and, for the case cited, the error would be about two degrees with a 30-degree angle between the measured wind direction and the line of sight. If winds were weaker or measured at a higher altitude, the direction error

would increase. The converse is also true. In normal practice the wind direction and speed are read off a plotting board. Those errors have not been considered here although the total error in direction may be as large as five degrees with a weak wind field. Until 1968 the wind direction was reported or coded for teletype transmission to the nearest 10 degrees so that it may usually be considered accurate to $\pm$ 5 degrees. Presently, the radiosonde code provides for reporting the wind direction to the nearest five degrees.

## IV. USEFULNESS OF VARIOUS ANALYSES AND COMPUTATIONS ON A MESOSCALE

Reduction of the rawinsonde data gathered in the NSSL Oklahoma mesonetwork was accomplished by computer. The program used was essentially the same as briefly described by Kreitzberg and Brockman (1966). The pressure data were automatically smoothed by a (1, 2, 1) weighting of the log of pressure according to $\ln P(m) = \left[ (\ln P(m-1) + 2\ln P(m) + \ln P(m+1) \right] / 4$. The heights of constant-pressure surfaces in 50 mb increments from 950 mb were computed hydrostatically, but the heights of contacts, other isobaric levels, and isentropic levels were all computed by interpolation from the 50 mb incremented levels assuming that the temperature varied with $P^{0.286}$ or that the lapse rate was dry adiabatic. Computer processing would induce less computational error than the graphical techniques used on the synoptic scale, and the computer output certainly provides more data than synoptic reports.

In analyzing mesoscale features one does not expect the gradients to be linear. However, in the absence of known trends or data to the contrary it is difficult to justify a nonlinear analysis. The amount of smoothing that is commonly done on a synoptic scale map to account for "bad" data is not possible on a mesoscale because the features to be analyzed may be obliterated. Therefore the initial analyses are the result of linear interpolations of the data assuming all the data are correct. Some revised analyses are also discussed in the subsections to follow.

At the time of the soundings considered, 1700Z on 28 May 1967, there were no thunderstorms observed in the NSSL mesonetwork, and none developed

until after the soundings were terminated. A weak surface stationary front was shown in the northwest corner of the area at 1800Z by Fankhauser (1969) but there is no indication of a front at 850 mb at this map time.

The station model used on the maps is:

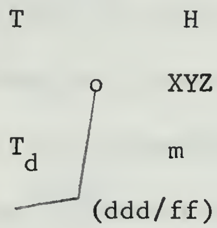


where temperature (T) and dew point ($T_d$) are reported to the nearest 0.1C; XYZ is station identification; H is height to the nearest meter; m is mixing ratio in gm $kgm^{-1}$; and ddd/ff is direction to the nearest degree and speed to the nearest meter per second.

## A. HEIGHT ANALYSIS

For synoptic scale data the heights of standard isobaric surfaces are normally analyzed with 30-, 60-, and 120-meter differences between isohypes with contour interval increasing with altitude. The 850-mb surface is usually analyzed with 30-meter increments while pressure levels above 850 mb and below 100 mb are analyzed at 60-meter intervals. If one assumes standard deviations of height differences between radiosondes to be 3, 10, and 20 meters at 850, 500, and 300 mb respectively, then the standard deviation of height differences range from one tenth to one third of the isohypse spacing and apparent inaccuracies can easily be smoothed. However, for the mesoscale case, the heights must be analyzed with a 10-meter difference between isohyses to get adequate definition. At 850 mb this should not be too bad, but at 300 mb the expected RMS error in height is twice as large as the isohypse interval.

In Figures 2a, b, and c the height analysis was done with the primary aim of drawing to the height data. Of secondary importance was making the contours fit the wind field. As a result of drawing to reported heights, the wind over at least part of all three maps may be described as antibaric. Furthermore, as one proceeds from the 850-mb through 500-mb to the 300-mb maps, the antibaric flow becomes more pronounced. The observed wind field does not justify any closed centers on any of these maps; but, to provide any resolution, one is obliged to draw contours at about 10-meter intervals, and the height data forces the closed centers at 500 mb and 300 mb.

The maximum height difference between stations on the 850-mb map is 21 meters; at 50 mb, 25 meters; and at 300 mb, 34 meters. If one considers the geostrophic wind equation

$$V_g = \frac{g}{f}\frac{\partial z}{\partial n} \tag{12}$$

and the height gradient between RIN and FSI on each of the three maps, then the geostrophic component of the wind normal to a line connecting these two stations would be 29, 33, and 37 m sec$^{-1}$ at 850, 500, and 300 mb, respectively. Obviously the wind is not geostrophic as there is at least some curvature to the streamlines; and, at 300 mb, a definite trough is evident near the middle of the map. Furthermore, one would expect some accelerations to be present in an area where thunderstorms develop a few hours after map time. The height differences between FSI and RIN are clearly excessive; and, from the analyses, one would suspect that FSI was reporting heights which were too low while RIN was reporting heights which were slightly too high. Similar comparisons may be made with other stations.

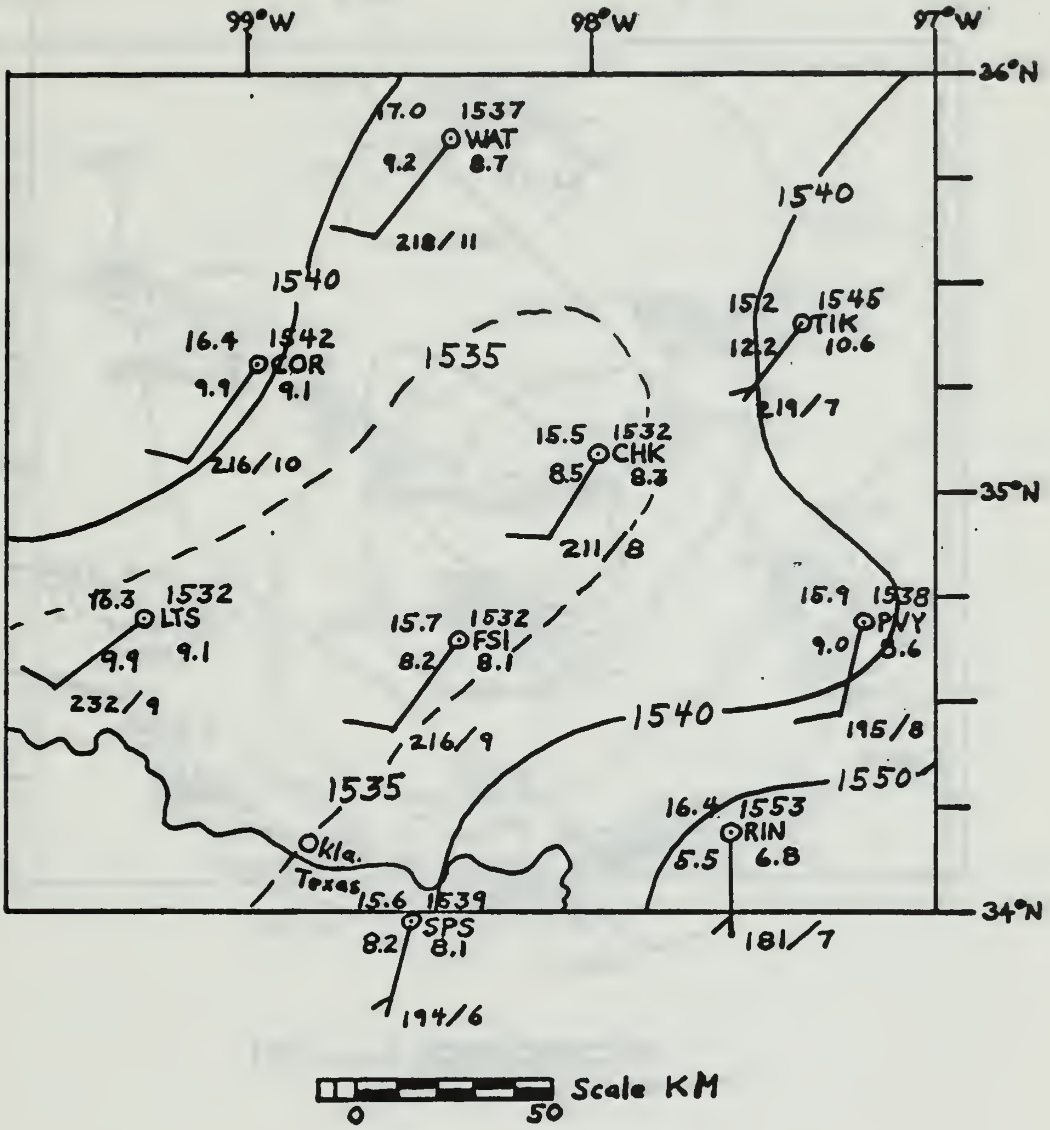


Figure 2a: 850 mb Height Analysis, 1700Z, 28 May 1967.

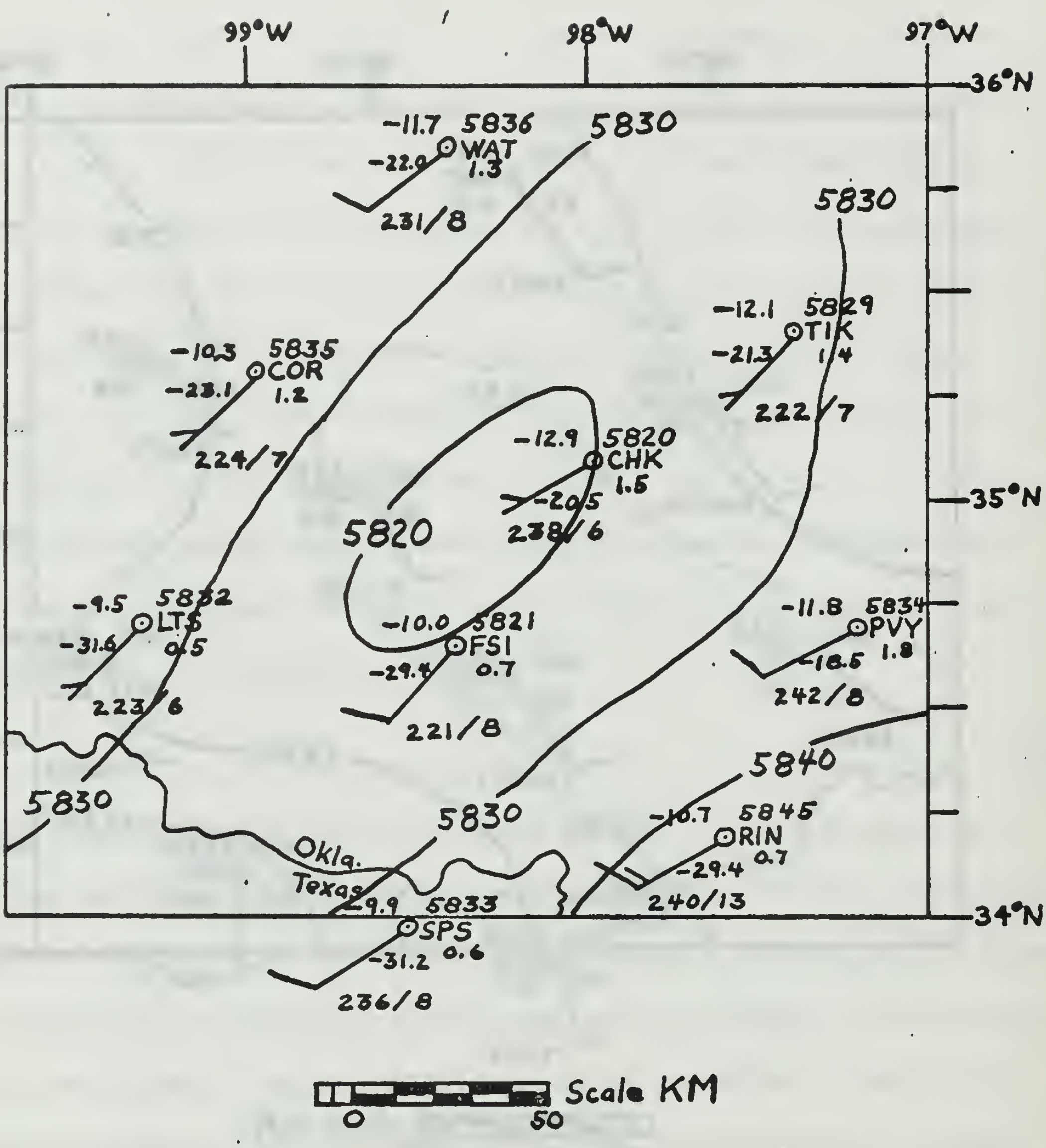


Figure 2b: 500 mb Height Analysis, 1700Z, 28 May 1967.

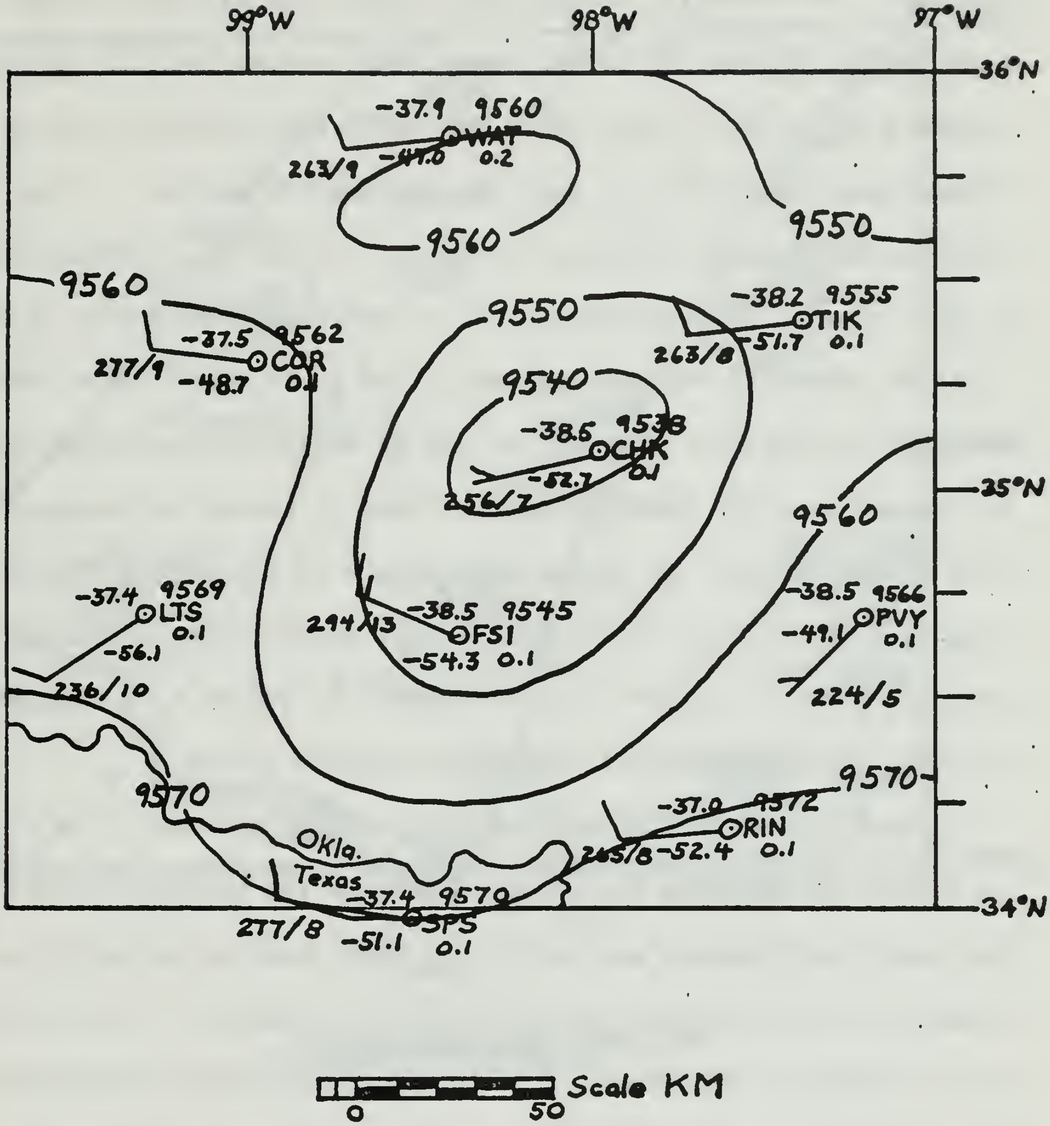


Figure 2c: 300 mb Height Analysis, 1700Z, 28 May 1967.

Even though the wind cannot be described as geostrophic on these maps, the geostrophic assumption does provide a starting point for analysis. Accordingly, the contour spacing for adjusted height analyses at 850 and 300 mb was computed from equation (12) using observed winds for $V_g$ and a five-meter interval between contours. Streamlines were used as a guide in placing the contours. These adjusted analyses are Figures 2d and 2e. At 850 mb, differences in height between the two analyses are 10 meters or less while at 300 mb up to 20 meters difference is found. One would expect from Table VI that RMS differences in height at 850 mb would be about three meters; but from this 1700Z data, it appears that $\sigma_h$ should be somewhere around five or six meters. Of course, there is a 5% chance that the difference will exceed $2\sigma_h$. At higher levels, standard deviations in heights given in Table VI appear to be accurate. At 300 mb $\sigma_h = 19.1$ meters, and this is compatible with observed apparent errors.

Synoptic-scale height analysis of isobaric surfaces in mid-latitudes is a means of defining the pressure systems and the wind field. With the dense data network available over North America and with the RMS relative errors less than half the contour interval, it is relatively easy to obtain a good analysis and adequately portray the synoptic situation. However, for this mesoscale case, the height analysis adds nothing to the understanding of the situation. At 500 mb the expected RMS relative error in reported height is the same magnitude as the necessary contour interval, and the situation worsens with increasing altitude. To assume that the winds are parallel to the height contours is a completely erroneous assumption. In fact, the height analysis in the middle and upper troposphere does nothing but confuse the situation. Streamlines or trajectories would be much more helpful.

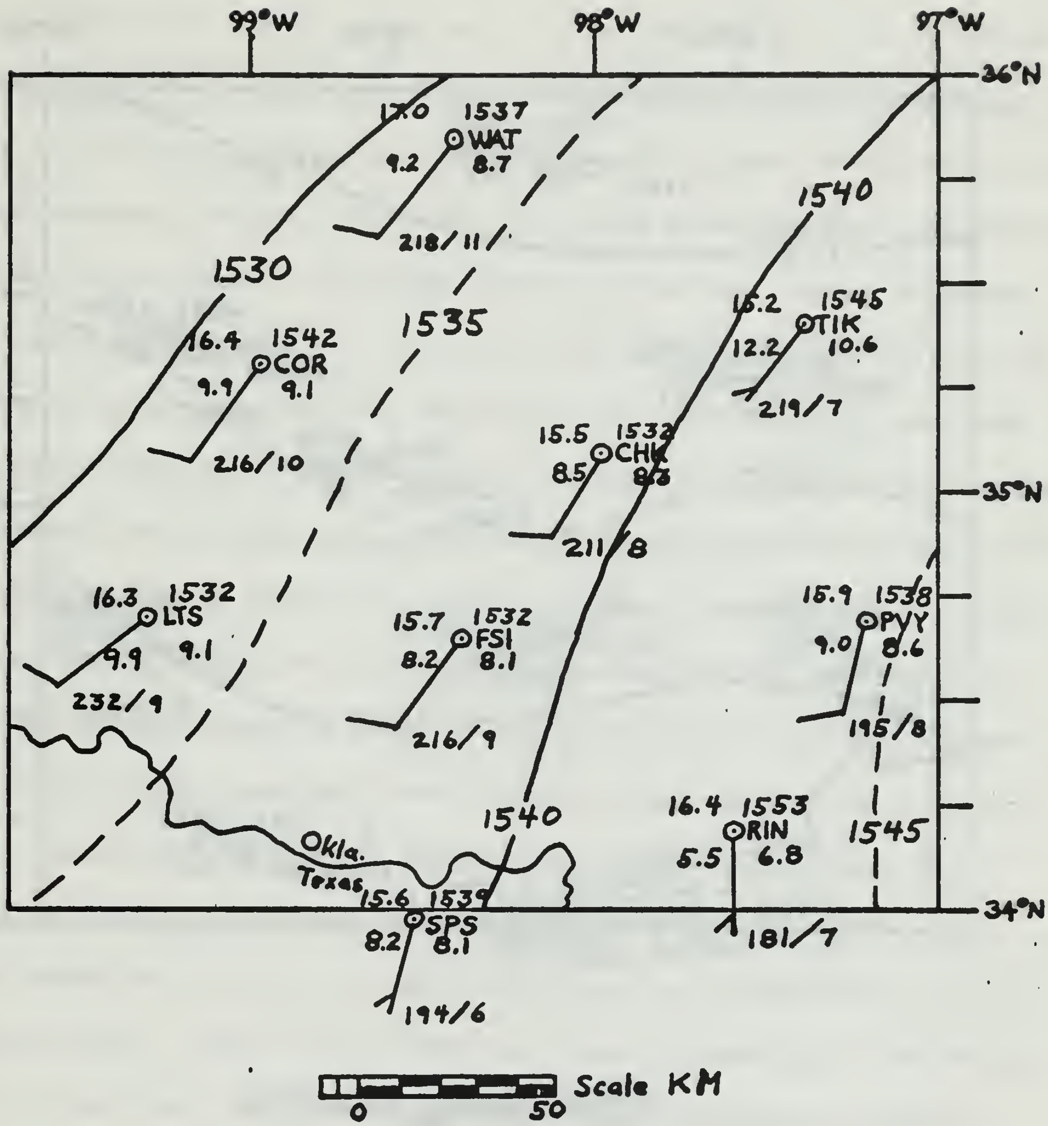


Figure 2d: Adjusted 850 mb Height Analysis, 1700Z, 28 May 1967. Isohypse spacing is based upon observed winds and the geostrophic assumption.

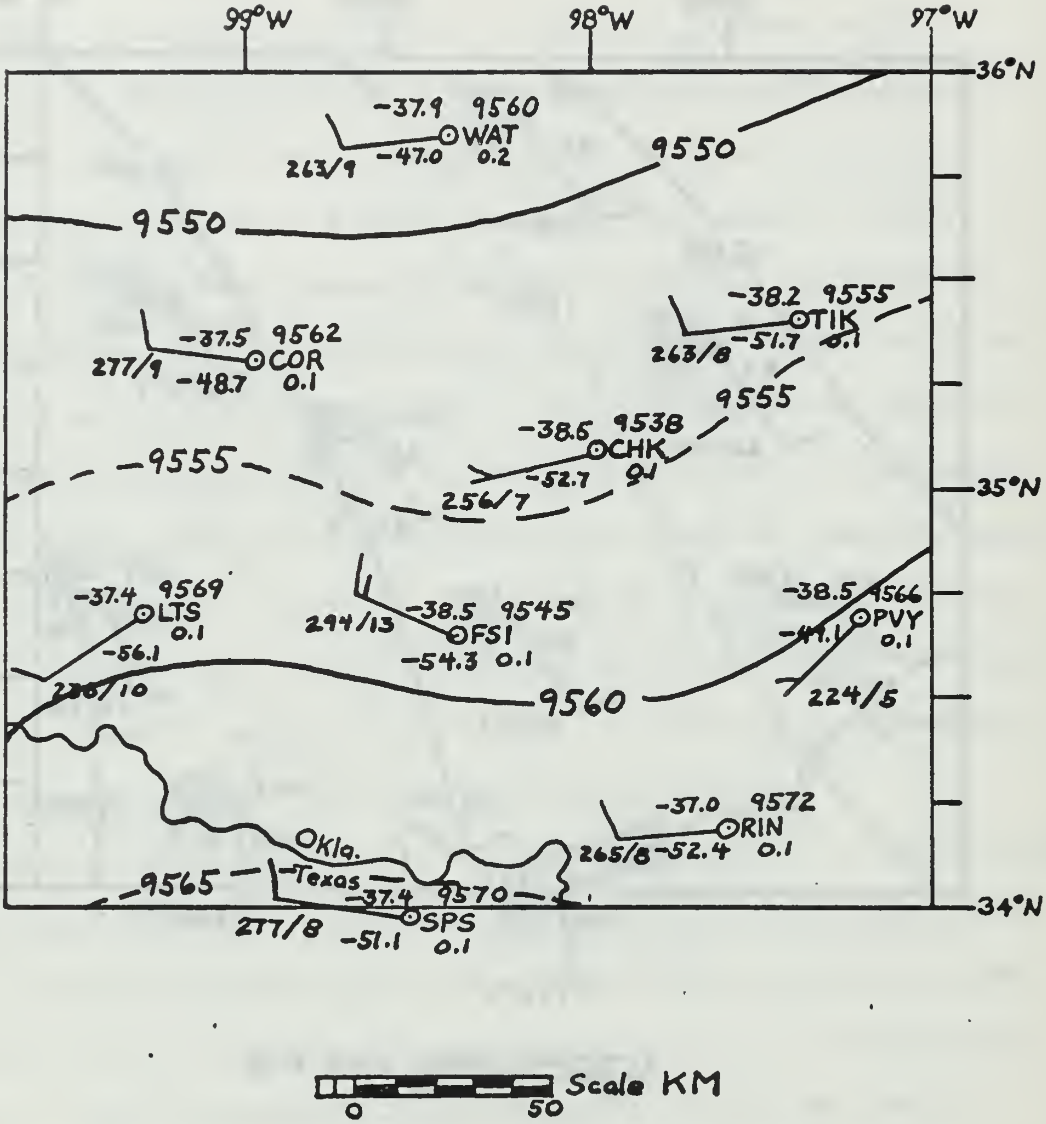


Figure 2e: Adjusted 300 mb Height Analysis, 1700Z, 28 May 1967. Isohypse spacing is based upon observed winds and the geostrophic assumption.

## B. TEMPERATURE ANALYSIS

The maximum temperature difference across the network for the 1700Z 28 May 1967 data is 1.8C at 850 mb, 3.4C at 500 mb, and 1.5C at 300 mb corresponding to $2.6\sigma$, $4.9\sigma$ and $2.1\sigma$ respectively. Here $\sigma$ is assumed to be $\pm$ 0.7C on a constant-pressure surface. As shown in Figure 3a, the 850-mb isotherm pattern indicates a cool area averaging about 15.6C from southwest to northeast across the middle of the map. These isotherms are nearly aligned with the wind field. At 300 mb (Figure 3c) four out of five of these stations are enclosed by the -38C isotherm, and much of the thermal gradient is oriented with the wind. In contrast to the 850- and 300-mb levels where temperature differences were rather slight, the 500-mb isotherms in Figure 3b reveal the large thermal gradient between FSI and CHK of 2.9C in 60 kilometers. How much of this difference is real and how much relative error is open to question. If one accepts $\sigma$ to be 0.7C, then this difference between adjacent stations would be $4.1\sigma$. Therefore, most of the thermal gradient is either real or a result of reading the wrong ordinate value into the raw data. The latter would be a result of a gross error and not considered a part of relative error. There were no observed clouds extending to the 500-mb level at that time and none of the radiosondes encountered clouds or precipitation on their ascent. Therefore, radiation and conduction errors of the two thermistors should have been equal and not been the cause of this tight gradient. If one neglects the temperature report at CHK, a smaller and more realistic thermal gradient results (see Figure 3d).

There is little qualitative use made of a temperature analysis on this scale. One may notice, however, that the wind does veer considerably

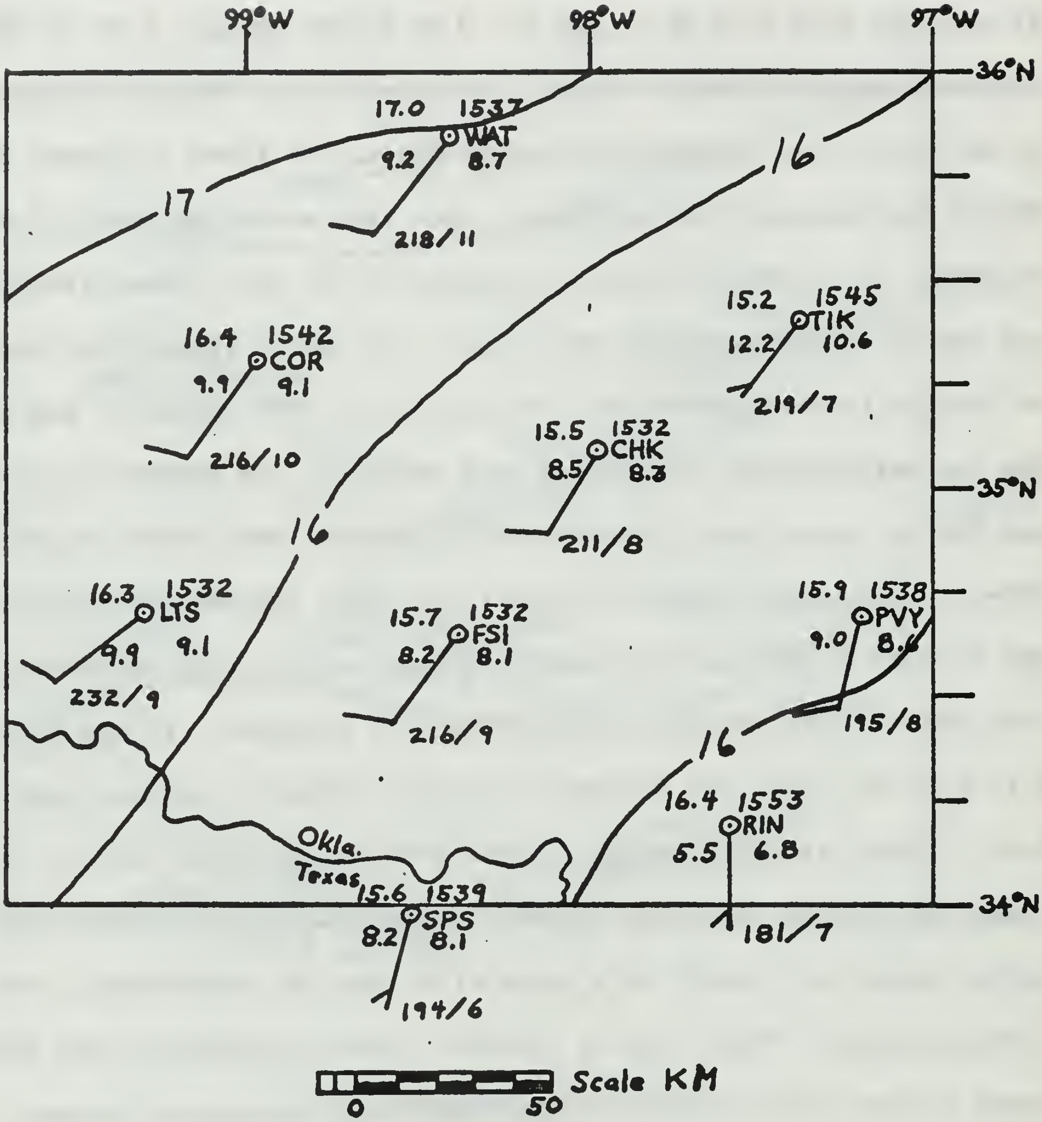


Figure 3a: 850 mb Temperature Analysis, 1700Z, 28 May 1967.

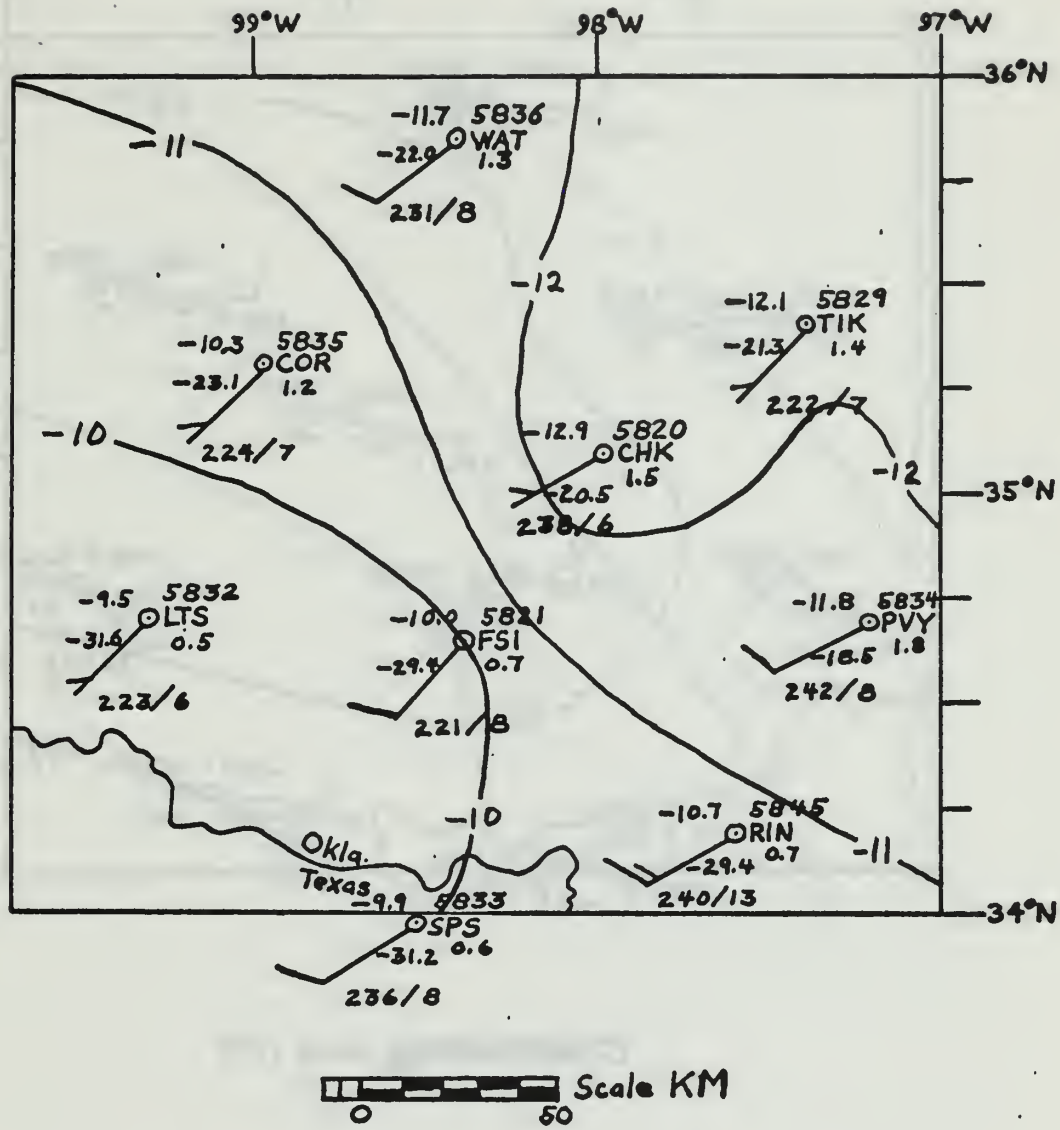


Figure 3b: 500 mb Temperature Analysis, 1700Z, 28 May 1967.

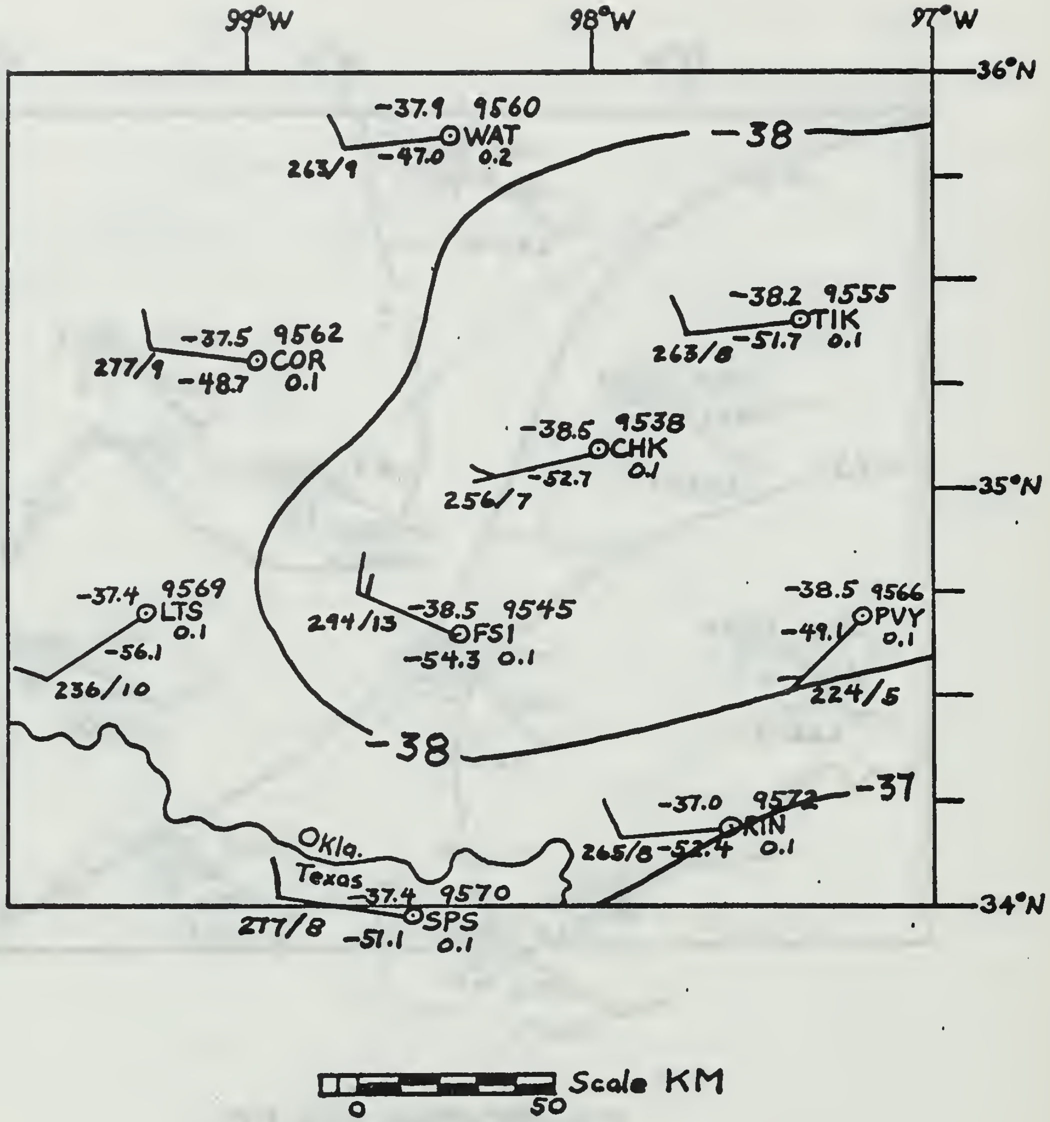


Figure 3c: 300 mb Temperature Analysis, 1700Z, 28 May 1967.

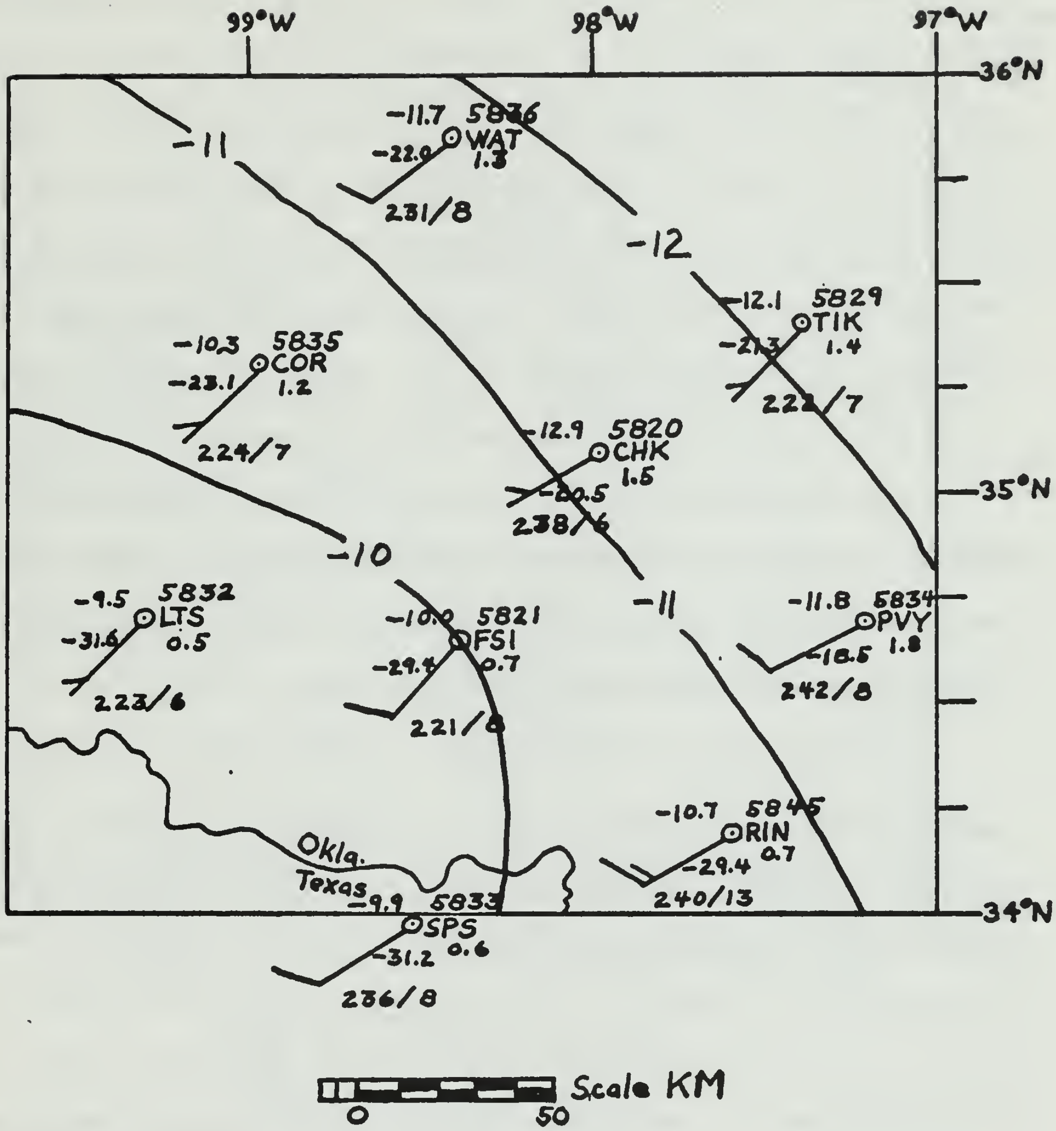


Figure 3d: Adjusted 500 mb Temperature Analysis, 1700Z, 28 May 1967. This analysis neglects the reported temperature at station CHK. Compare with Figure 3b.

between 500 mb and 300 mb, and in particular the wind change at FSI shows the effect of warm advection. There are two computer outputs in the single-sounding program which might at first glance use temperature data. Static energy will be considered in a latter section. The advective temperature change is not computed by using observed temperatures but by use of observed winds and the thermal wind relationship assuming that the variation of observed wind with height is the same as the variation of geostrophic wind. Kreitzberg and Brockman (1966) indicate that good results were obtained by this method in Project Stormy Spring.

Most advective temperature changes (ATC) as computed from the thermal wind relationship and at all layers and stations were less than 0.5C per hour. If one compares the winds, temperatures, and distance between FSI and CHK at 500 mb, a much larger figure would be expected. From the definition of positive temperature advection,

$$ATC = - \mathbb{V} \cdot \nabla_p T, \tag{13}$$

the result, using a wind speed of seven meters per second, is +1.22C per hour. Equation (13) may be written in natural coordinates as $ATC = - V \frac{\partial T}{\partial s}$. Differentiating for error analysis yields:

$$d(ATC) = - d(V) \frac{\partial T}{\partial s} - V \frac{\partial (dT)}{\partial s}, \tag{14}$$

where d(ATC) may be equated to RMS error in temperature advection as computed from the values at an isobaric surface; the first term on the right side, the error due to wind speed and direction; and the second, the error due to temperature. For example, disregard the reported temperature at CHK and consider only the gradient shown in Figure 3d where the average distance between isotherms is about 55 km. If one assumes the RMS error in wind speed to be one meter per second, $\sigma_{TP}$

to be 0.7C, and the average wind from FSI to TIK to be seven meters per second, then the expected RMS error in temperature advection due to error in wind speed would be 0.065C per hour while that due to error in temperature would be 0.32C per hour. Combining the two results, assuming that the errors are independent of each other, would yield a total error in ATC of 0.33C per hour. The total expected RMS error for this example is mostly caused by the error in temperature and is the same order of magnitude as the results using the computer program. The maximum ATC for this area of +0.25C per hour occurred at TIK in the 500-450 mb layer.

## C. MOISTURE ANALYSIS

Measurements of moisture content are essential to the understanding and prediction of convective storms. While the analysis of moisture parameters at standard isobaric surfaces is of little use in itself, mixing ratio is often used in computing static and total energy, diabatic heating, and stability, to name a few. Water vapor is undoubtedly the most variable of all atmospheric constituents, and its measurement is the least accurate. To investigate how well the water vapor content can be defined on this scale, analyses of moisture parameters were attempted at 850, 500, and 300 mb and are listed as Figure 4a, 4b, and 4c respectively.

At 850 mb the mixing ratio analysis provides a pattern in which one may have confidence. The assumed standard deviation in reported mixing ratio for this level is about 0.6 gm $kgm^{-1}$. Dew points for this level were also analyzed, but the error in dew point varies more from station to station and depends not only upon temperature but upon relative humidity as well. Although the RMS error in dew point does not vary

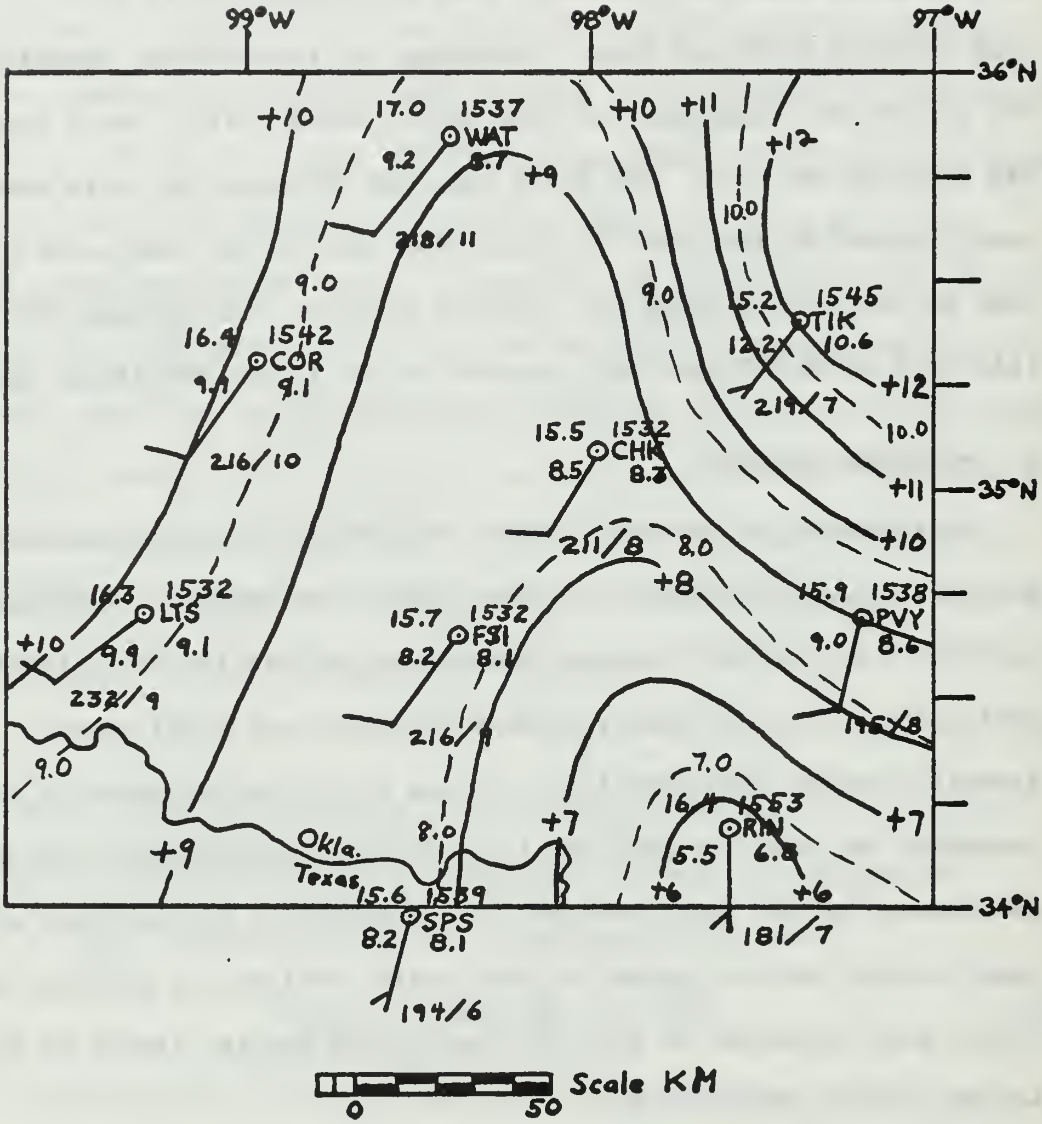


Figure 4a: 850 mb Dew-point and Mixing Ratio Analysis, 1700Z, 28 May 1967.

Mixing Ratio - - - - -

Dew Point ——————

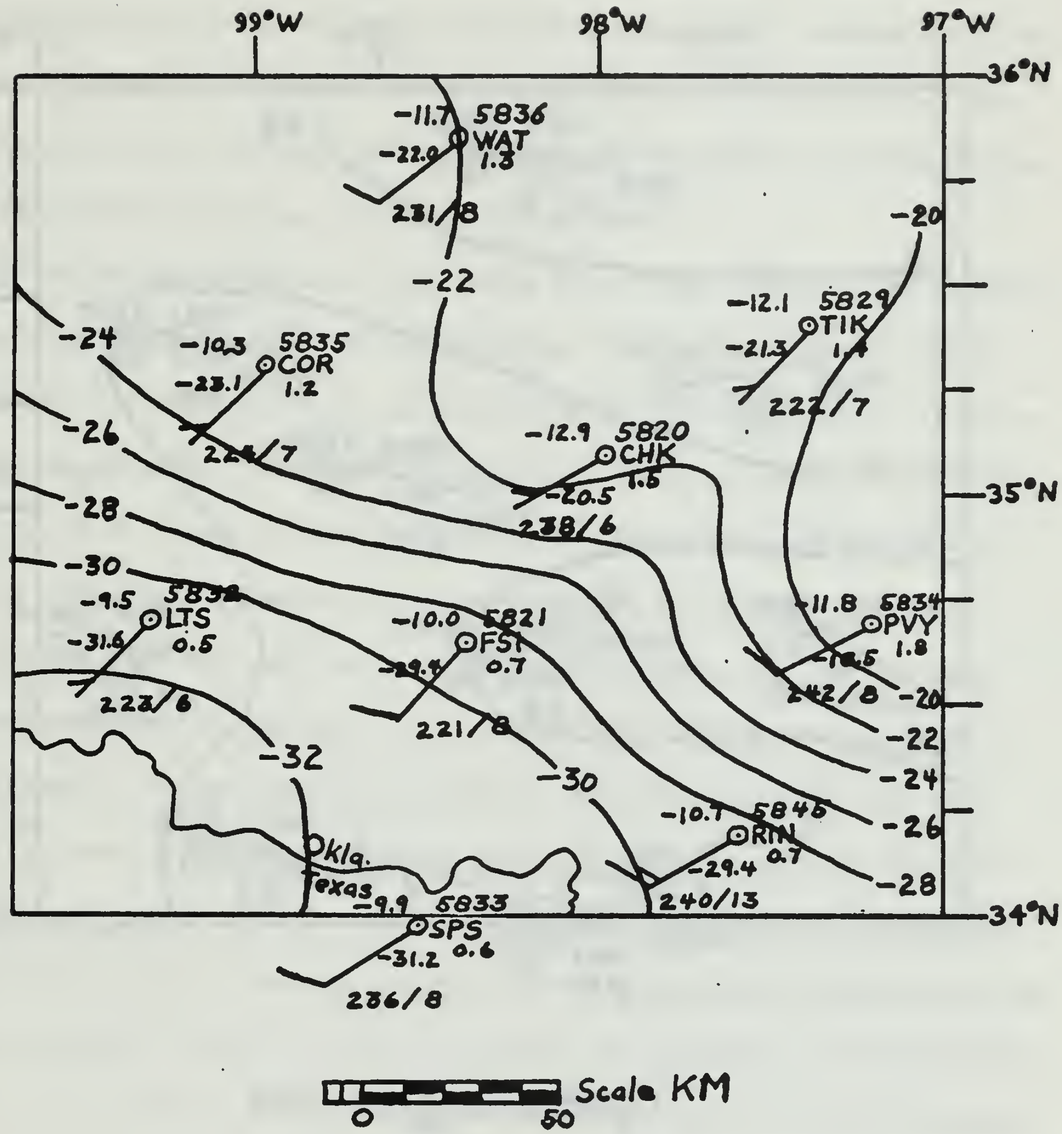


Figure 4b: 500 mb Dew-point Analysis, 1700Z, 28 May 1967.

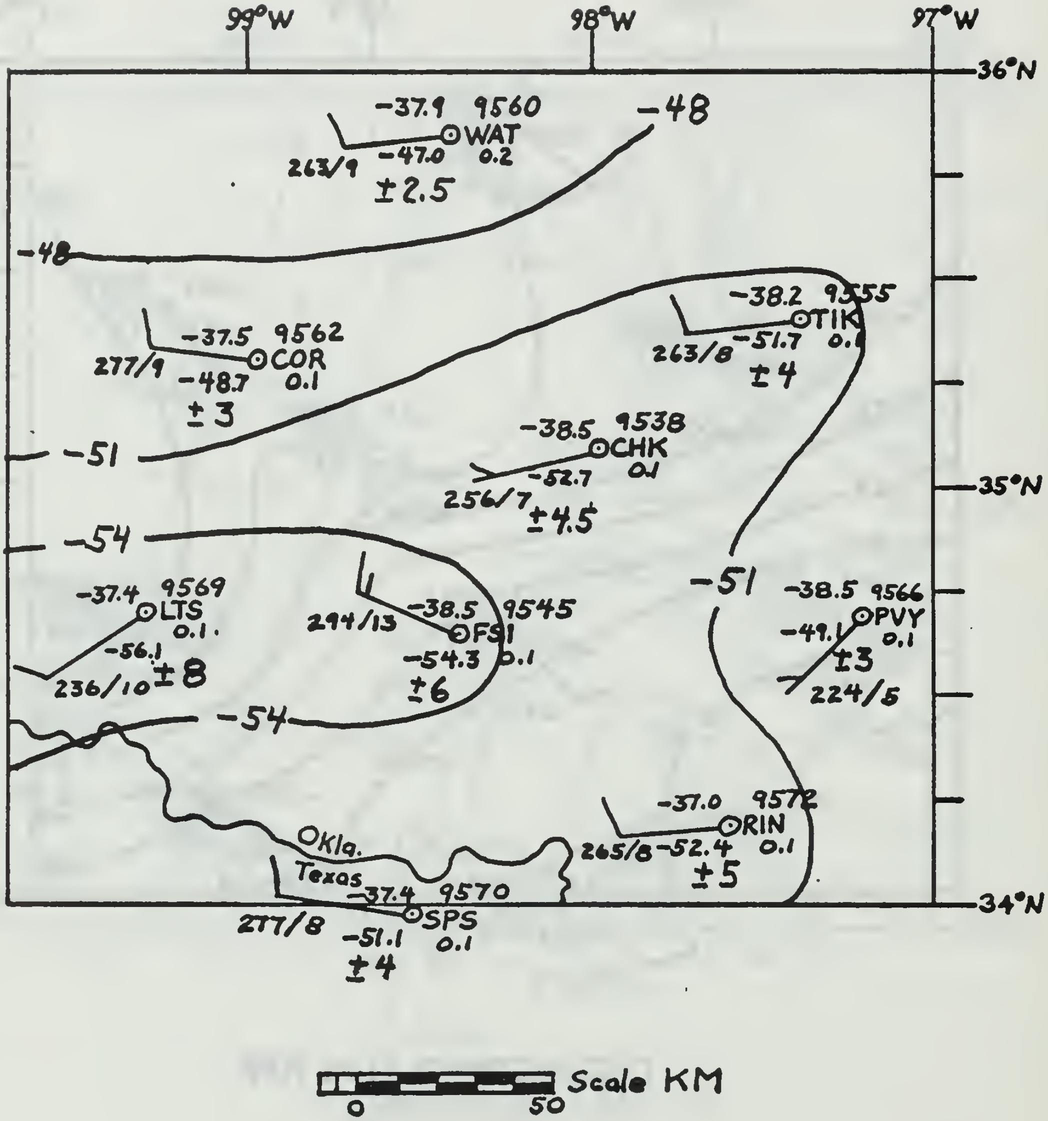


Figure 4c: 300 mb Dew-point Analysis, 1700Z, 28 May 1967. Numbers under the dew-points at each station are expected RMS errors in dew-point.

inversely with the realtive humidity as does the RMS error in <u>reported</u> relative humidity, it does vary at about the same rate. That is, if relative humidity decreases at a constant pressure and temperature, the spread (in degrees centigrade) represented by $\pm$ $0.1m_s$ increases. The maximum difference of dew point values at 850 mb across the network was 6.7C while that of mixing ratio was 3.8 gm $kgm^{-1}$.

By 500 mb the temperature was below 0C so that expected RMS relative errors of $\pm$ 10% relative humidity applies. This translates to about 0.3 gm $kgm^{-1}$ in mixing ratio corresponding to $m_s$ = 3.0 gm $kgm^{-1}$ for the average temperature found at this level. Although isopleths of mixing ratio could be drawn, better definition is obtained by analyzing dew points. Therefore only dew point isopleths at two-degree intervals were drawn, but they must be interpreted with caution. The accuracy of the dew points so analyzed vary considerably and are not related to an arbitrarily chosen isopleth interval. Whether comparing mixing ratios or dew points, it is obvious that the eastern edge of the area contains more water vapor than the south-western corner. The expected RMS relative error in mixing ratio remains essentially the same over the entire map and is equal to 10% of $m_s$ which is dependent upon temperature. However, the expected standard deviation in dew point is also dependent upon relative humidity and varied from about $\pm$ 8C at LTS to $\pm$ 2C at PVY with relative humidity at these stations 15% and 60% respectively.

One glance at Figure 4c will indicate the necessity for analyzing dew points. The mixing ratio was reported as 0.1 gm $kgm^{-1}$ with the exception of station WAT which reported 0.2 gm $kgm^{-1}$. Relative humidity varied from about 15% to 35%. The resultant dew point RMS errors range

from ± 8C at LTS to ± 2.5C at WAT and are indicated at each station to the nearest half degree in Figure 4c.

Relatively accurate depiction of water vapor content on this scale is possible at lower levels with temperatures above 0C. In the middle and upper troposphere, errors are likely to be much larger although a qualitative judgement of the moisture content at the normal limiting temperature (-40C) seems possible. Relative humidity and dew point are available as computer output up to the limit of the sounding (100 mb) for this network, but standard practice in the synoptic network limits information on water vapor content to dew points at standard levels where temperature is greater than -40C.

## D. MESOSCALE WIND ACCURACY

Before discussing computations derived from analysis of the wind field some procedures used at NSSL in measurement and computation of the wind should be mentioned. Azimuth and elevation angles were recorded at 30-second intervals. There was a capability of recording these angles at six-second intervals, but this procedure was not used unless elevation angles were less than 12 degrees (Fankhauser, 1969). On 28 May 1967 the winds were rather light and would result in elevation angles on the order of 25 to 40 degrees. Kreitzberg and Brockman (1966) indicated that the data taken at 30-second intervals were not smoothed but three-point interpolation was used to yield azimuth and elevation angles at each contact base. The detailed wind at each contact over the curved earth was computed by centered differencing of the values at the contacts at either side which provided about a one-minute average. Then the mean winds, which were printed by the computer, were computed by a (1, 2, 1) weighted average of the detailed winds.

Since the winds at any particular point are the result of averaging over five or six elevation and azimuth angles, some of the random errors in measurement of GMD-1 angles should be averaged out. The accuracy of the reported winds should approach that which Danielsen and Duquet (1966) reported (about one m $sec^{-1}$ and two degrees for light winds).

## E. ENERGY COMPUTATIONS

Another computer output in the data supplied by NSSL is static energy at constant pressure levels which is defined as: $SE = c_p T + gz + Lm$. Total energy is also used and consists of static energy plus a kinetic energy term. Therefore, total energy is defined as:

$$TE = c_p T + gz + Lm + \frac{V^2}{2} \tag{15}$$

or

$$TE = 1.004T + 0.0098Z + 2500m + \frac{V^2}{2} \times 10^{-3} \tag{15a}$$

where T is in degrees Kelvin, z is in meters, m is mixing ratio in gm/gm, V is wind speed in m $sec^{-1}$ and TE is total energy in j $gm^{-1}$. At 500 mb (Figure 2b) average values of temperature, height, mixing ratio, and wind speed substituted into equation (15) would yield:

$$\begin{aligned} TE &= 1.004\ (263) + 0.0098\ (5830) + 2500\ (0.001) + \frac{(V)^2}{2} \times 10^{-3} \\ &= 264 + 57 + 2.5 + 0.025. \end{aligned}$$

Thus one can see that the terms in the equation are arranged in descending order of contribution to total energy.

The RMS error in total energy is composed of errors in all four parameters. The standard deviation in temperature is assumed to be 0.7C; height (at 500 mb), 10.6 meters; mixing ratio (at 500 mb), 0.0003; and wind speed, 1.0 m $sec^{-1}$. Therefore, the RMS error in the temperature

term is approximately 0.7; height term, 0.1; moisture term, 0.75; and kinetic energy term, 0.0005; all expressed in units of j $gm^{-1}$. The largest errors are contained in the temperature and moisture terms and are about equal in magnitude at 500 mb. However, the error in the moisture term at 850 mb would be twice as large as at 500 mb because $m_s \doteq 12.0$ gm $kgm^{-1}$ and therefore $\sigma_m = 0.6$ gm $kgm^{-1}$. The error in temperature is assumed to remain constant. If the errors in these four parameters are assumed independent of each other, the RMS error in total energy is given by:

$$\sigma_{TE} = \sqrt{(0.7)^2 + (0.1)^2 + (0.75)^2 + (0.0005)^2} = 1.03 \text{ j gm}^{-1}.$$

The total energy at 500 mb ranged from 322.8 j $gm^{-1}$ at RIN to 324.4 j $gm^{-1}$ at COR. The maximum difference of 1.6 j $gm^{-1}$ may be compared to the expected RMS error of 1.03 j $gm^{-1}$. The maximum change in total energy across the 500-mb map is so small relative to the RMS error that comparisons between stations are of questionable use in other than a qualitative way. At 850 mb, however, the maximum difference of 8.3 j $gm^{-1}$ is about five times as large as the expected RMS error for that level, and analysis at that level could be more revealing.

## F. ISENTROPIC TRAJECTORIES

The use of isentropic trajectories for the study of vertical motions, moisture sources, and accelerations, to name a few, has been widely accepted as a valuable synoptic-scale tool. The use of kinematic isentropic trajectories derived from NSSL mesonetwork data to study the meteorological properties of air parcels has been described by Van Sickle (1969). He adapted a computer program originated by Mahlman (1968) for use on this mesoscale to compute and draw these trajectories.

Nine other parameters were also computed at both ends of each trajectory but most will not be discussed here.

For synoptic scale work the Montgomery stream function (M) is invaluable in adjusting the trajectory at each time step. However, Van Sickle found that in many cases isopleths of M were perpendicular to the wind; and, therefore, he had to compute trajectories kinematically. Computer output of Montgomery stream function contains virtual temperature instead of air temperature; because the θ values were computed using virtual temperature, and the isentropic surfaces were really surfaces of constant potential virtual temperature. Thus the equations for M and θ become:

$$\theta_v = T_v \left(\frac{1000}{P}\right)^{0.286} \tag{16}$$

and

$$M = c_p T_v + gz = 1.004T_v + 0.0098z \tag{17}$$

where $T_v$ is in degrees Kelvin, z is height in geopotential meters above mean sea level, and M is in j $gm^{-1}$. Errors in temperature, pressure, and mixing ratio cause errors in both $\theta_v$ and M. It is safe to assume that these errors don't completely cancel each other so that there is some error in M on an isentropic surface. To make the values of M dynamically consistent with the winds and accelerations, Van Sickle had to make some rather large modifications of M relative to the total range of values across the mesoscale area. For example, on the θ = 320 surface which was at 500 $\pm$ 20 mb the values of M ranged from 320.70 to 321.05 j $gm^{-1}$ for a total spread of 0.35 j $gm^{-1}$. Yet modifications of up to 0.25 j $gm^{-1}$ or five times the isopleth interval were necessary to make the values of M consistent with observed winds and accelerations.

These modifications are equivalent to errors in temperature of 0.25C or 25 meters in height which represent $0.36\sigma_T$ and $0.8\sigma_z$ respectively.

Van Sickle (1969) also found that moisture content was a crucial factor in determining total energy on an isentropic surface. The contour patterns of total energy in his study closely resembled the mixing ratio field which indicates that the third term (Lm) dominates in both total and static energy. To change total energy by 1.0 j $gm^{-1}$ requires either a change in temperature of 1.0C, a change in height of 100 meters, a change in wind speed of 45 meters m $sec^{-1}$, or a change in mixing ratio of 0.4 gm $kgm^{-1}$. Obviously mixing ratio is the most sensitive and variable parameter. One could not expect either energy calculation to yield information which could be relied upon in other than a qualitative way.

Kinematic trajectories on isentropic surfaces have proved to be valuable in studying local storms. Vertical motions obtained by Van Sickle were consistent with the observed growth and decay of thunderstorms which occurred the afternoon of 28 May 1967 in the Oklahoma mesonetwork. Convergence and divergence of trajectories were consistent with storm location. Height and temperature inaccuracies in the Montgomery stream function rendered it useless for studies on this scale, and computations involving moisture content did not prove to be reliable. Analyses and computations based upon adequate description in time and space of the wind field were shown to be the most useful in this study.

## G. VORTICITY AND DIVERGENCE

One of the most useful tools in predicting cloudiness and precipitation is the knowledge of vorticity and divergence patterns. Several methods of computing vertical motion are based upon these quantities.

Coleman (1969) attempted to adapt these synoptic-scale techniques to the study of a squall line in the Oklahoma mesonetwork which occurred on 30 May 1967. From streamline and isotach analyses at each 50 mb interval in the troposphere he computed vorticity, divergence, and vertical motions.

Both divergence and vorticity contain terms involving spatial gradients of velocity. If wind speed is accurate to within one m $sec^{-1}$ and the average distance between stations is 85 km, then the RMS error in these terms are on the order of $10^{-5}$ $sec^{-1}$. Coleman found divergences from $10^{-5}$ to $10^{-4}$ $sec^{-1}$ and relative vorticities from $10^{-5}$ $sec^{-1}$ up to a maximum of 50 x $10^{-5}$ $sec^{-1}$ near the squall line. In some areas the computed divergences and vorticities were of the same order of magnitude as the RMS error,but near the squall line these computed quantities were at least one order of magnitude larger than the error.

The vertical motions were obtained by two different schemes. One was based upon a vorticity relationship while the other was based upon divergence. The vertical motion computer program based upon vorticity did not converge because the advection term was too large due to very tight spatial gradients. This program had been successfully utilized for synoptic-scale studies. The divergence-derived vertical motion program revealed maximum vertical velocities of about 100 mb $hr^{-1}$.

It is interesting to note that Coleman did not intentionally smooth the wind data in the initial analyses. The winds on 30 May for the area were approximately twice the magnitude of winds on 28 May and averaged about 20 meters per second at 500 mb and 30 m $sec^{-1}$ near the tropopause. There was some averaging done after the initial computation of vorticity

and divergence. This smoothing amounted to giving the grid point in question on the pressure surface 40% weight and the four surrounding grid points 15% each. Vertical smoothing was accomplished by a (1, 2, 1) weighted average. The reported winds, of course, represent a weighted average over about 600 meters.

This appears to be another method which can be successfully used for further understanding of severe local storms. Its validity is dependent upon the accuracy of the wind data and streamline and isotach analyses. The winds seem to provide the most reliable and useful information at constant-pressure surfaces for studies of this scale of motion.

## V. CONCLUSIONS

RMS errors between radiosondes assumed for both measured and derived parameters seem to have been borne out by several meteorologists who have analyzed the NSSL data. The minimum RMS relative error in height of standard pressure surfaces is probably about five meters but those derived for the middle and upper troposphere seem to be consistent with results. One would expect that radiosonde data from the synoptic network would contain slightly larger relative errors due to increased variability in the exposure of the instruments and the use of graphical techniques for data reduction.

Wind accuracy on the synoptic scale is highly variable as outlined in Section IIIE. Errors in balloon position and therefore computed winds are directly correlated with wind speed, altitude, slant range, and elevation angle. By computer processing and successive averaging of GMD-1 angles and detailed winds the mesoscale wind data appears to contain much less error than one would expect from synoptic-scale experience.

Rawinsonde-derived data from the synoptic network are adequate to portray cyclones and other meteorological events of similar size. This is possible because the RMS relative errors are small relative to the magnitude of the meteorological changes encountered, and the data density in the continental United States is adequate for the task. Height fields, thermal advection, stability indices, and vorticity patterns are primary tools for the forecaster. However, on a mesoscale the RMS relative errors in height, temperature, and moisture parameters are too large

relative to maximum differences observed across the mesoscale network to be useful. The amount of smoothing necessary to achieve reliable analyses appears to be the same order of magnitude as the respective RMS errors. Comparison of original and adjusted height fields confirms this although there is no direct comparison possible for other parameters.

The wind data appears to contain the most useful information. The problem in isotherm analysis and thermal advection has been surmounted by computing advective temperature change utilizing observed winds and the thermal wind relationship. Streamlines and isotachs may be substituted for the more conventional height analysis for depiction of the wind field on isobaric surfaces. Kinematic trajectories on isentropic surfaces over short (1.5 hours) periods of time are another means of describing the wind field. Both methods lead to computation of vorticity, divergence, and vertical motion all of which are essential to the understanding of thunderstorm dynamics.

It would be most helpful if the measurement of water vapor content in the atmosphere were accurate enough to rely upon for quantitative analyses and computations of energies, diabatic heating, and the like. Some of the inherent errors in mixing ratio may be eliminated by using values which are averaged over 50 mb layers (cf. Frankhauser, 1969). One may attempt calculations of total moisture inflow into a squall line by advecting these mean values with the mean wind in each 50 mb layer. Nevertheless, there will always be considerable error in reported moisture parameters as long as either the lithium chloride or the carbon element are used. The former element is reluctant to measure high relative humidities while the latter will not measure low relative

humidities. An element which is more sensitive with an RMS error of about 0.1 gm $kgm^{-1}$ in mixing ratio is badly needed for both routine radiosonde use and detailed mesoscale investigations.

## VI. SUGGESTIONS FOR IMPROVEMENT IN RAWINSONDE ACCURACY

The most important improvement to be made in radiosonde accuracy is to get a better humidity element in routine use. Large scale air-sea interaction studies would be possible and diabatic heating could be studied with some accuracy over land. A better sensor is even more important for mesoscale studies. For several years barium flouride and aluminum oxide elements have been under development by the National Bureau of Standards and Air Force Cambridge Research Laboratories, respectively. Both featured fast response times, and early reports were encouraging ( cf. Jones (1963); Chleck (1966)). However, Brousaides (1968) has concluded that the aluminum oxide element is not suitable for radiosonde use because of large hysteresis, small resistance change with relative and specific humidity, and temperature dependence. The barium flouride element has been found to lack the desired stability in storage. It might be worth the cost and effort if a batch were manufactured, calibrated, and used as an experiment in the NSSL network. Failing that, an accurate aircraft borne sensor could be employed for mesoscale research.

The next improvement in rawinsonde data in order of priority should be observed winds. It is obvious that if precision radars, such as the FPS-16, are available for balloon tracking, they should be used. However, it is unlikely that such radars will be available in sufficient quantity in the next decade or so. The next best approach would be the use of a transponder-radiosonde such as that developed by the Weather Bureau which is capable of being used with the new GMD-2 tracking

equipment. Either way, position errors in range are always less than errors in slant range; whereas, with the present system, errors in height of the radiosonde are magnified in range by multiplying by the cotangent of the elevation angle.

Errors in temperature and height would be next in line for improvement. A shielded bead thermistor could be suspended from an outrigger attached to the radiosonde as a replacement for the presently used rod thermistors. This would decrease solar radiation and conduction errors as well as reducing response time. These errors are particularly important in the stratosphere, but it is felt that relative errors could also be reduced in the troposphere with corresponding decreases in RMS errors in height of isobaric surfaces if data reduction were accomplished by computer. Smaller decreases in these height errors would be realized if the graphical technique were used. Camp and Caplan (1969) investigated temperature errors of a bead thermistor which was mounted on a JIMSPHERE and compared with standard radiosonde measurements. The bead thermistor showed faster response and more detail throughout each flight and considerably less total error at altitudes above 11 km.

If angular measurements and slant range of a transponder-radiosonde system were sufficiently accurate (equivalent to the FPS-16), it would be practical to compute height using range and elevation angle. Height analysis for mesoscale studies would again be feasible. In addition, pressure could be computed from height and temperature data more accurately than it is now measured with the baroswitch. These methods of obtaining heights and pressures would be particularly valuable at altitudes above 700 mb.

BIBLIOGRAPHY

Air Weather Service Pamphlet 105-3, Environmental-Measuring Equipment Used by Air Weather Service in Support of Air Force and Army Operations, 10 November 1967 (AD-822895).

Air Weather Service Technical Report 105-133, Accuracies of Radiosonde Data, September 1955.

Anawalt, LT R. A., USN, An Approach to the Numerical Modelling of Cumulus-Scale Motions, Masters Thesis, Naval Postgraduate School, Monterey, California, 1969.

Andersen, LT R. T., USN, Thermal Effects on Baroswitches, Bachelor's Research Paper, Naval Postgraduate School, Monterey, California, 1966.

Badgley, F. I., "Response of Radiosonde Thermistors," The Review of Scientific Instruments, v. 28, p. 1079-1084, December 1957.

Brousaides, F. L., An Evaluation of the Aluminum Oxide Humidity Element, AFCRL-68-0547, Instrumentation Papers, No. 151, October 1968.

Camp, D. W. and F. E. Caplan, "High Resolution Balloonborne Temperature Sensor," Journal of Applied Meteorology, v. 8, p. 159-166, February 1969.

Chleck, D., "Aluminum Oxide Hygrometer: Laboratory Performance and Flight Results," Journal of Applied Meteorology, v. 5, p. 878-886, December 1966.

Coleman, LT R. J., USN, A Diagnostic Analysis of the 30 May 1967 Squall Line in Central Oklahoma, Masters Thesis, Naval Postgraduate School, Monterey, California, 1969.

Corbeille, LT R. C., USN, An Experimental Investigation of Radiosondes, Masters Thesis, Naval Postgraduate School, Monterey, California, 1966.

Daniels, G. E., "Errors of Radiosonde and Rocketsonde Temperature Sensors," Bulletin of the American Meteorological Society, v. 49, p. 16-18, January 1968.

Danielsen, E. F. and R. T. Duquet, A Comparison of FPS-16 and GMD-1 Measurements and Methods for Processing Wind Data, NASA Contractor Report CR-61158, 66 p., 28 November 1966.

Dowski, E. R., High-Altitude Hypsometer Radiosonde Tests, U. S. Army Signal Research and Development Laboratory Technical Report 2242, December 1961.

Fankhauser, J. C., Convective Processes Resolved by a Mesoscale Rawinsonde Network, paper presented at the Sixth Conference on Severe Local Storms, April 1969.

Ference, J. Jr., "Instruments and Techniques for Meteorological Measurements," Compendium of Meteorology, p. 1207-1222, American Meteorological Society, 1961.

Haltiner, G. J. and F. L. Martin, Dynamical and Physical Meteorology, McGraw-Hill, 1957.

Hodge, M. W. and C. Harmantas, "Compatability of United States Radiosondes," Monthly Weather Review, v. 93, p. 253-266, April 1965.

Jones, F. E., "Performance of the Barium Flouride Film Hygrometer Element on Radiosonde Flights," Journal of Geophysical Research, v. 68, p. 2735-2751, 1 May 1963.

Jones, F. E. and A. Wexler, "A Barium Flouride Film Hygrometer Element," Journal of Geophysical Research, v. 65, p. 2087-2095, July 1960.

Kreitzberg, C. W. and W. E. Brockman, Computer Processing of Mesoscale Rawinsonde Data from Project Stormy Spring, AFCRL-66-97 Special Reports, No. 41, February 1966.

Lhermitte, R. M., Note on Probing Balloon Motion by Doppler Radar, National Severe Storms Laboratory Technical Memorandum No. 34, p. 1-13, July 1967.

MacCready, P. B. Jr., "Comparison of Some Balloon Techniques," Journal of Applied Meteorology, v. 4, p. 504-508, August 1965.

Mahlman, J. D., Numerical Methods of Computing Three-Dimensional Trajectories for Adiabatic and Diabatic Flows, AFCRL Report No. 68-0357, 1968.

Mathews, D. A., "Review of the Lithium Chloride Radiosonde Hygrometer," Humidity and Moisture, v. 1, p. 219-227, Reinhold, 1964.

McVehil, G. E., R. J. Pilié, and G. A. Zigrossi, "Some Measurements of Balloon Motions with Doppler Radar," Journal of Applied Meteorology, v. 4, p. 146-148, February 1965.

Mitchell, L. V., Radiosonde Dew-Point Accuracies 40C to -40C, Air Weather Service Technical Report 198, 20 October 1967. (AD-659760)

Murrow, H. N. and R. M. Henry, "Self-Induced Balloon Motions," Journal of Applied Meteorology, v. 4, p. 131-138, February 1965.

Ney, E. P., R. W. Mass, and W. F. Huch, "The Measurement of Atmospheric Temperature," Journal of Meteorology, v. 18, p. 60-80, February 1961.

O'Connor, LCDR J. F., USN, Practical Methods of Weather Analysis and Prognosis, p. 32, NavAer 50-1P-502, U. S. Navy, 1952.

Reynolds, R. D. and R. L. Lamberth, "Ambient Temperature Measurements from Radiosondes Flown on Constant-Level Balloons," Journal of Applied Meteorology, v. 5, p. 304-307, June 1966.

Scoggins, J. R., "Spherical Balloon Wind Sensor Behavior," Journal of Applied Meteorology, v. 4, p. 139-145, February 1965.

Smith, L. G., A Study Comparing Winds Aloft Measuring Equipment at Salton Sea Test Base, Sandia Corporation Technical Report No. 3512, 9 November 1954.

Van Sickle, LT K. L., USN, A Kinematic Isentropic Trajectory Study of a Local Severe Storm, Bachelor's Research Paper, Naval Postgraduate School, Monterey, California, 1969.

## INITIAL DISTRIBUTION LIST

| | | No. Copies |
|---|---|---|
| 1. | Lieutenant Commander Bruce A. Clark, USN<br>USS MIDWAY (CVA-41)<br>c/o San Francisco Bay Naval Shipyard<br>San Francisco, California 94135 | 3 |
| 2. | Professor R. L. Alberty<br>Department of Meteorology<br>Naval Postgraduate School<br>Monterey, California 93940 | 5 |
| 3. | Professor C. L. Taylor<br>Department of Meteorology<br>Naval Postgraduate School<br>Monterey, California 93940 | 5 |
| 4. | Commanding Officer<br>Fleet Numerical Weather Center<br>Monterey, California 93940 | 1 |
| 5. | Professor R. Panholzer<br>Department of Electrical Engineering<br>Naval Postgraduate School<br>Monterey, California 93940 | 1 |
| 6. | Commander, Naval Weather Service Command<br>Naval Weather Service Headquarters<br>Washington Navy Yard<br>Washington, D. C. 20390 | 1 |
| 7. | Mr. Herbert Keel<br>Geophysics Division<br>Pacific Missile Range<br>Point Mugu, California 93041 | 1 |
| 8. | Defense Documentation Center<br>Cameron Station<br>Alexandria, Virginia 22314 | 20 |
| 9. | Library<br>Naval Postgraduate School<br>Monterey, California 93940 | 2 |
| 10. | Department of Meteorology<br>Naval Postgraduate School<br>Monterey, California 93940 | 2 |

11. Commanding Officer 2
Naval Weather Research Facility
Naval Air Station, Building R-48
Norfolk, Virginia 23511

12. Commander 1
Naval Air Systems Command
Headquarters
Washington, D. C. 20360

Security Classification

## DOCUMENT CONTROL DATA - R & D

*(Security classification of title, body of abstract and indexing annotation must be entered when the overall report is classified)*

| | |
|---|---|
| 1. ORIGINATING ACTIVITY *(Corporate author)*<br>Naval Postgraduate School<br>Monterey, California 93940 | 2a. REPORT SECURITY CLASSIFICATION<br>Unclassified<br>2b. GROUP |

3. REPORT TITLE

Rawinsonde Errors and Their Application to a Mesoscale Study

4. DESCRIPTIVE NOTES *(Type of report and inclusive dates)*

Master's Thesis; October 1969

5. AUTHOR(S) *(First name, middle initial, last name)*

Bruce Alan Clark

| 6. REPORT DATE | 7a. TOTAL NO. OF PAGES | 7b. NO. OF REFS |
|---|---|---|
| October 1969 | 80 | 33 |

| | |
|---|---|
| 8a. CONTRACT OR GRANT NO. | 9a. ORIGINATOR'S REPORT NUMBER(S) |
| b. PROJECT NO. | |
| c. | 9b. OTHER REPORT NO(S) *(Any other numbers that may be assigned this report)* |
| d. | |

10. DISTRIBUTION STATEMENT

This document has been approved for public release and sale; its distribution is unlimited.

| 11. SUPPLEMENTARY NOTES | 12. SPONSORING MILITARY ACTIVITY |
|---|---|
| | Naval Postgraduate School<br>Monterey, California 93940 |

13. ABSTRACT

Several studies of rawinsonde component errors in actual flight tests are discussed. RMS relative errors between radiosondes are assumed for measured parameters. These errors are then used to derive RMS relative errors for other parameters such as wind speed and direction, height, virtual temperature, and mixing ratio. Expected RMS errors in measured and derived parameters are discussed in relation to the data obtained from the Oklahoma National Severe Storms Laboratory upper-air mesonetwork. It is found that many analyses and computations which are useful in synoptic-scale meteorology are not practical on the mesoscale. Wind data, when processed by computer, yield the most valid results.

DD FORM 1 NOV 65 1473 (PAGE 1)

S/N 0101-807-6811



Security Classification

A-31408

| 14 KEY WORDS | LINK A | | LINK B | | LINK C | |
|---|---|---|---|---|---|---|
| | ROLE | WT | ROLE | WT | ROLE | WT |
| Data accuracy | | | | | | |
| Mesoscale analyses | | | | | | |
| Rawinsonde errors | | | | | | |